FISEVIER

Contents lists available at ScienceDirect

### Earth and Planetary Science Letters

www.elsevier.com/locate/epsl



## Holocene glacier behavior around the northern Antarctic Peninsula and possible causes



M.R. Kaplan  $^{a,*}$ , J.A. Strelin  $^{b,c}$ , J.M. Schaefer  $^{a,d}$ , C. Peltier  $^{a,d}$ , M.A. Martini  $^{c,e,f}$ , E. Flores  $^c$ , G. Winckler  $^{a,d}$ , R. Schwartz  $^a$ 

- <sup>a</sup> Geochemistry, Lamont-Doherty Earth Observatory, Palisades, NY 10964, USA
- <sup>b</sup> Instituto Antártico Argentino, Argentina
- <sup>c</sup> Centro de Investigaciones en Ciencias de la Tierra (CICTERRA, CONICET-Facultad de Ciencias Exactas, Físicas y Naturales, UNC), Córdoba, Argentina
- <sup>d</sup> Department of Earth and Environmental Sciences, Columbia University, New York, NY 10027, USA
- e Núcleo Milenio Paleoclima, Universidad de Chile, Santiago, Chile
- f Instituto de Geografía, Pontificia Universidad Católica de Chile, Santiago, Chile

#### ARTICLE INFO

# Article history: Received 19 September 2019 Received in revised form 21 December 2019 Accepted 6 January 2020 Available online xxxx Editor: L. Robinson

Keywords:
Antarctic Peninsula
cosmogenic dating
deglaciation
Holocene
Antarctica
paleoclimate

#### ABSTRACT

We obtained 49 new  $^{10}$ Be ages that document the activity of the former Northern Antarctic Peninsula Ice Sheet, and subsequently the James Ross Island Ice Cap and nearby glaciers, from the end of the last glacial period until the last  $\sim$ 100 years. The data indicate that from >11 to  $\sim$ 8 ka marked recession of glacier systems occurred around James Ross Island, including tidewater and local land-terminating glaciers. Glaciers reached heads of bays and fjords by 8-7 ka. Subsequently, local glaciers were larger than present around (at least) 7.5-7 ka and  $\sim$ 5-4 ka, at times between 3.9 and 3.6 ka and just after 3 ka, between  $\sim$ 2.4 and  $\sim$ 1 ka, and from  $\sim$ 300 to  $\sim$ 100 years ago. After deglaciation, the largest local glacier extents occurred between  $\sim$ 7 ka and  $\sim$ 4 ka.

Comparison with other paleoclimate records, including of sea ice extent, reveals coherent climate changes over  $\sim 15^\circ$  of latitude. In the early Holocene, most of the time a swath of warmth spanned from southern South America to the Antarctic Peninsula sector. We infer such intervals are times of weakening and/or poleward expansion of the band of stronger westerlies, associated with contraction of the polar vortex. Conversely, increased sea ice and equatorward expansion of the westerlies and the polar vortex favor larger glaciers from Patagonia to the Antarctic Peninsula, which typically occurred after  $\sim 8$  ka, although warm stretches did take place. For example, on the Antarctic Peninsula and in Patagonia the interval from 4 to  $\sim 3$  ka was typically warm, but conditions were not uniform in either region. We also infer that reduced and expanded glacier extents in Patagonia and the eastern Antarctic Peninsula tend to occur when conditions resemble a persistent positive and negative southern annular mode, respectively.

© 2020 Elsevier B.V. All rights reserved.

#### 1. Introduction

This study aims to improve understanding of past glacier behavior around the northern Antarctic Peninsula and associated climates, regionally and across the middle to high latitudes of the Southern Hemisphere. Observations on glacier behavior since the end of the last glacial period can provide a long-term context for the prominent cryosphere changes observed over the last few decades (e.g., Davies et al., 2014), in part, by evaluating past glacier sensitivity to climate change. Knowledge of former glacier activity

around the northern Antarctic Peninsula also may provide insights into past climates that affected the larger cryosphere farther to the south.

Specifically, we seek to address (at least) the following outstanding questions. Following deglaciation, what was the timing of retreat of glaciers into fjords, embayments, and onto land? After, during the Holocene, when were glaciers larger than present and when were they generally reduced in extent? Furthermore, can we use the glacier record to improve understanding of past millennial shifts in the globally important Southern Westerly Winds and persistent patterns of the Southern Annular Mode (SAM)?

To address such questions concerning past glacier and climate history, we obtained new <sup>10</sup>Be ages on James Ross Island, Long Island, and Seymour Island (Figs. 1, 2). We build on pioneer-

<sup>\*</sup> Corresponding author.

E-mail address: mkaplan@ldeo.columbia.edu (M.R. Kaplan).

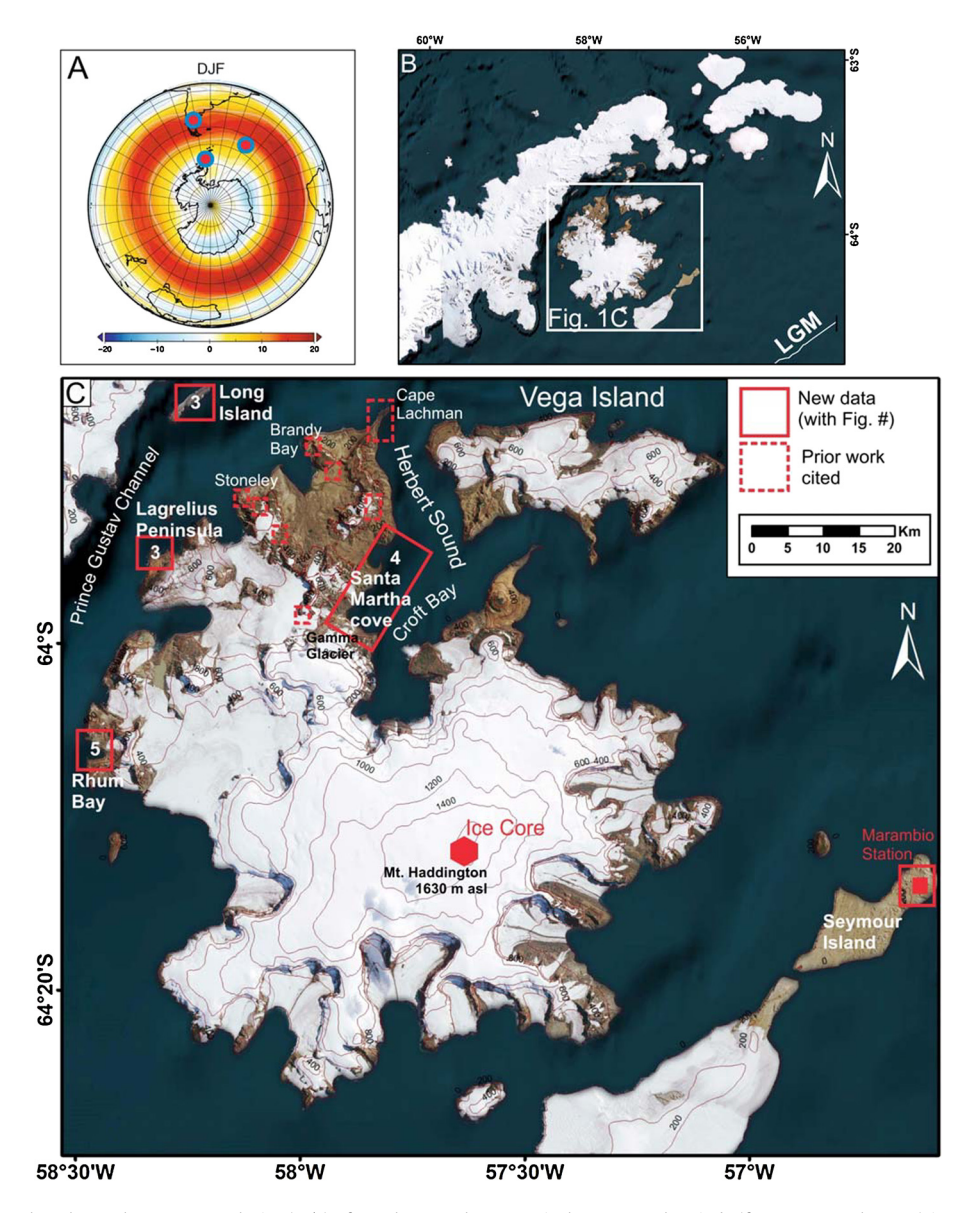


**Fig. 1.** A) A polar projection that shows the summer velocity (m/s) of 700 hPa Southern Hemisphere Westerly winds (from Moy et al., 2009) in southern South America and Antarctica. The three red/blue circles mark records shown in Fig. 6. The records span  $\sim$ 15 degrees of latitude. B) Image showing location of James Ross and Long Islands. C) Places mentioned in the text, including on Figures. Dashed rectangles surround areas on James Ross Island where ages (discussed in this paper) are from prior publications. Base images are from Bing Maps. (For interpretation of the colors in the figure(s), the reader is referred to the web version of this article.)

ing studies by others around area of James Ross Island (Fig. 1) (Zale and Karlen, 1989; Ingólfsson et al., 1992; Björck et al., 1996; Hjort et al., 1997; 1998; Strelin et al., 2006; Bentley et al., 2009; Johnson et al., 2011; Davies et al., 2014; Balco et al., 2013; Glasser et al., 2014; Nývlt et al., 2014; Jeong et al., 2018). Prior studies on James Ross Island and surrounding areas based on 10 Be dating have tended to focus (although not exclusively) on the last deglaciation and subsequent retreat onto land (e.g., Johnson et al., 2011; Balco et al., 2013; Glasser et al., 2014; Nývlt et al., 2014; Ó'Cofaigh et al., 2014; Jeong et al., 2018). The past studies have provided critical insights on former deglaciation of the Antarctic Peninsula Ice Sheet and neighboring ice shelves. Here, we provide new <sup>10</sup>Be chronologies of local glacier changes around James Ross Island during the Holocene, including a novel dataset for the last few hundred years, in addition to building on understanding of the last deglaciation. We then compare the <sup>10</sup>Be-based findings from the northern Antarctic Peninsula with recently obtained records in southern Patagonia and the Southern Ocean. We use the regional perspective to address the question of how past cryospheric changes around the northern Antarctic Peninsula may relate to the Westerly Winds and climatic patterns (e.g., SAM).

#### 2. Background and methods

Glaciers on James Ross Island are particularly sensitive to climate. This includes summer temperature (Davies et al., 2014) because — unlike almost all of Antarctica — temperatures in the glacier sole may oscillate around or above the freezing point for extended periods, leading to a polythermal regime (Chinn and Dillon, 1987). This thermal regime can strongly influence glacier mass balance, in part, because sustained summer temperatures oscillating around (or above) freezing can cause significant melting and sublimation, especially when dry northwest Chinook-like winds occur.

We sampled for cosmogenic nuclide dating in 2013 and 2014 (Figs. 1, 2). The dating effort is tied to geomorphic mapping (Figs. 3, 4), which is based on extensive field investigations over the last two decades (Strelin, unpublished observations; Strelin and Malagnino, 1992; Strelin et al., 2006) and the use of aerial photos.

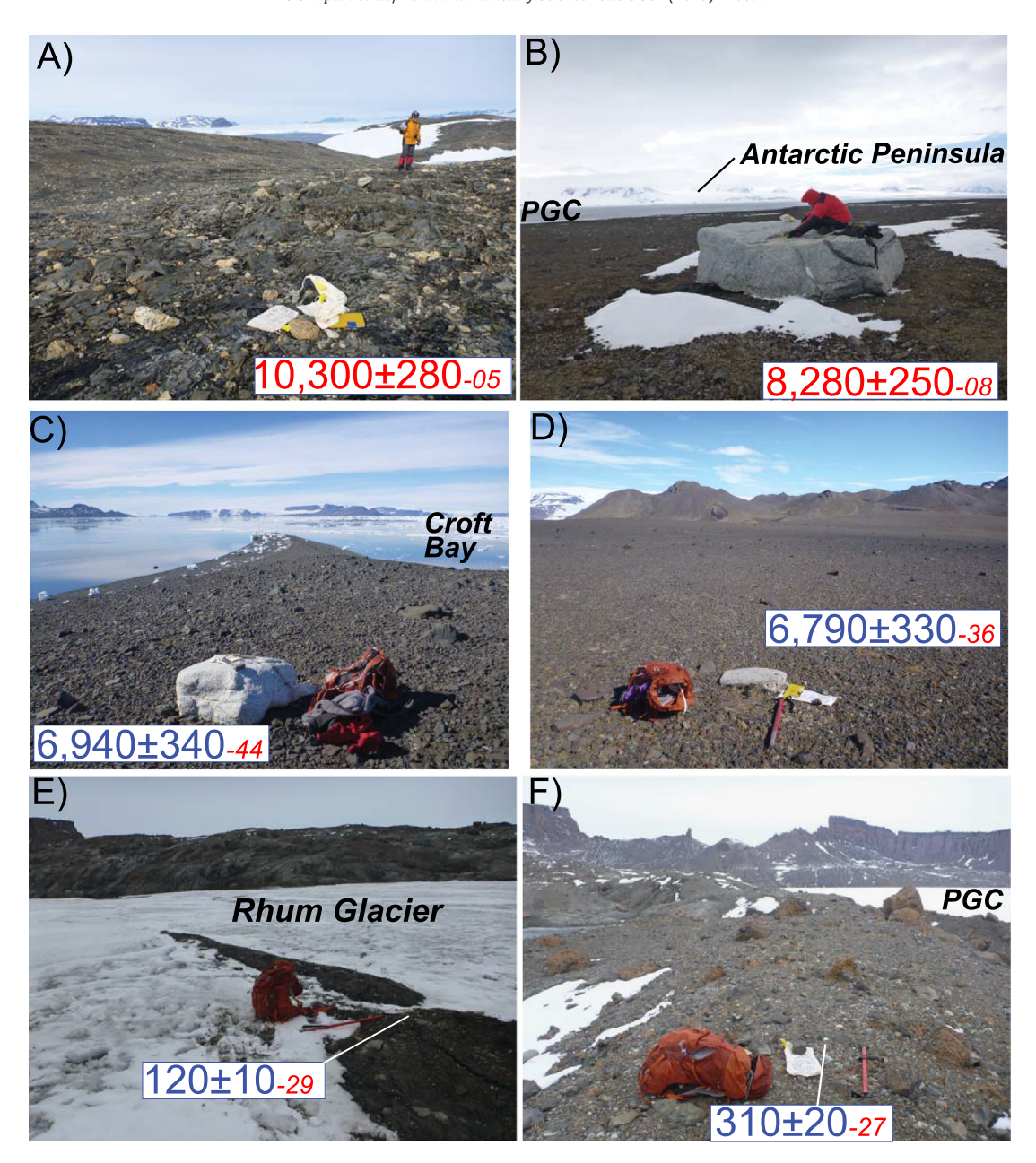


**Fig. 2.** Photos of samples, with the last two digits after each age referring to the label (Tables S1, S2). Red and blue labels represent erratics left behind as ice ablated and moraine samples, respectively, following the convention used throughout the paper. A) Cobble left behind on Long Island, with view of James Ross Island in background; B) Large erratic on Lagrelius Peninsula; C) Moraine boulder in the Dreadnought area; D) Moraine boulder at Santa Martha, with view looking south, toward higher parts of moraine where other samples are located (Fig. 4); E) <sup>10</sup>Be dated cobble-size stone from a debris band sitting on top of the ice close to the glacier front (Fig. 5); we assume it reflects surface lowering over the last few decades or century, causing emergence of the upward-flowing englacial or subglacial till layers. F) <sup>10</sup>Be dated cobble-size stone on one of the outer moraines fronting the Rhum glacier (Fig. 5A, B). PGC=Rhum Bay which opens to the Prince Gustav Channel. All photos taken by Kaplan.

We present the first data sets from field localities on the western and southwestern side of James Ross Island, including Long Island, which is within 5 km of the Antarctic Peninsula, Lagrelius Peninsula, and the Rhum and Dreadnought areas (Figs. 1–3). For post-LGM fluctuations, we mainly focus on local glacier systems that terminated on land, such as the Rhum and Alpha valleys (Figs. 1, 3).

The <sup>10</sup>Be samples came from cobbles on bedrock or boulders embedded in the crests of ground or lateral moraine ridges that appear stable. We sampled primarily quartz-rich granites or metamorphic lithologies (schists with quartz veins) derived from the Andean Granite Suite and Trinity Peninsula Group of the Antarctic Peninsula, respectively; these exotic erratics may have been carried by the last Antarctic Peninsula Ice Sheet that covered the area,

or alternatively, reworked from older (late Miocene to Pleistocene) tills that are ubiquitous throughout James Ross Island (Strelin and Malagnino, 1992; Smellie et al., 2008; Davies et al., 2012). We also sampled four sandstone erratics derived from local Cretaceous marine deposits of the Marambio Group; three from the Santa Martha-Alpha Glacier area and one from Dreadnought Peninsula (Fig. 4). In addition, to document changes over the last few centuries and to evaluate the possible magnitude of inheritance of cosmogenic nuclides in glacier deposits in the study area, we obtained samples from deposits formed during recent glacier fluctuations.

We were careful to collect samples above recorded local Holocene marine limits, in places up to  $\sim\!20$  m above present sea level. Samples were taken with a hammer and chisel from the up-

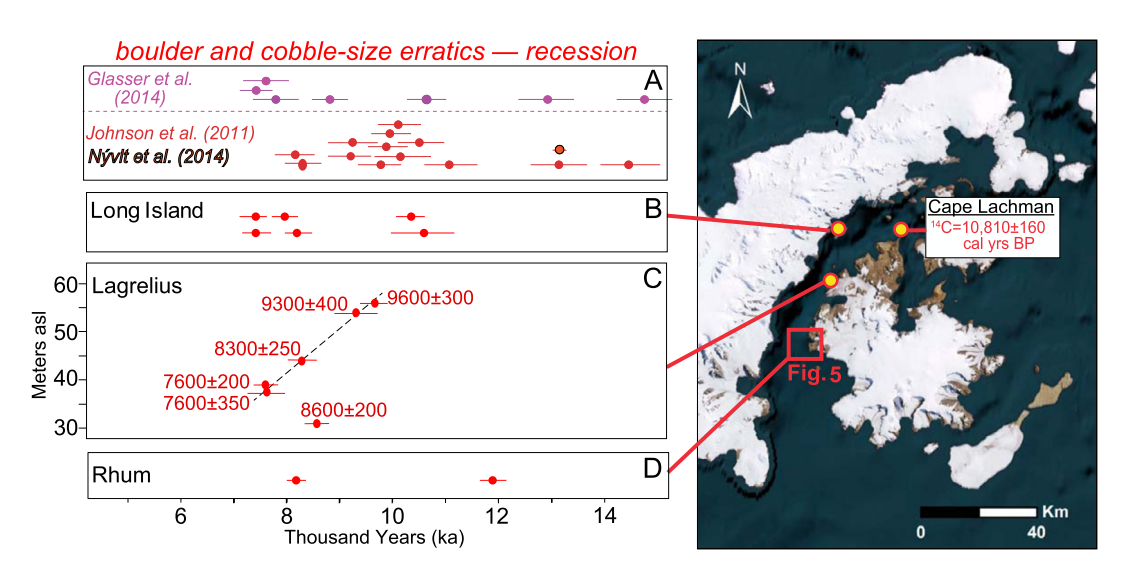


**Fig. 3.** New  $^{10}$ Be ages on erratics and cobbles from western/southwestern James Ross Island and Long Island, and ages obtained in prior studies from the same general area. **A)**  $^{10}$ Be ages obtained previously on James Ross and Seymour Islands (Fig. 1, Table S3); Fig. 1 shows the field sites. Only ages <14 ka are shown (see text); **B)** Long Island, where ages show a bimodal distribution,  $\sim$ 11-10 (n=2) ka and  $\sim$ 8-7 (n=4) ka. This island is  $\sim$ 3-4 km east of the Antarctic Peninsula; **C)** Lagrelius Peninsula, where there is an apparent trend of decreasing age towards elevation; **D)** The Rhum site, where we obtained only two deglacial ages (Fig. 5). We note that all new  $^{10}$ Be ages are generally consistent with data from prior studies (panel A). On right side, we also show the  $^{14}$ C age for initial deglaciation, from Ingólfsson et al. (1992).

per 1-3 cm of the most stable and flat section of the boulder top, or an entire cobble (e.g., Long Island). We used a handheld Garmin GPS to measure position and altitude, relative to the WGS 1984 datum, and a compass and clinometer to record azimuthal elevations of the surrounding landscape. In addition, at Dreadnought, we used a hand level to measure sample elevation above mean high tide (see Supplementary Material, Table S1). In some places, as a check on elevations, we used a Trimble ProXH differential GPS system, relative to the WGS 1984 datum; differential and handheld GPS measurements at the same location agree within  $\sim\!5$  m for longitude and latitude, and from 1 to 8 m for altitude (average difference is  $\sim\!3$  m).

We followed standard geochemical processing protocols (e.g., Schaefer et al., 2009) at the Cosmogenic Nuclide Laboratory at the Lamont-Doherty Earth Observatory. If cobbles were larger than needed, we sawed them in such a way so that the thickness of cobble remained intact; that is, we sawed the samples and then crushed a top-to-bottom piece. AMS measurement was at the Center for Accelerator Mass Spectrometry (CAMS) at Lawrence Livermore National Laboratory. Recent developments enable measurement of <sup>10</sup>Be concentrations of only 10<sup>3</sup> atoms/g (Schaefer et al., 2009), such as in this study.

<sup>10</sup>Be ages are calculated based on the methods incorporated in the CRONUS-Earth online exposure age calculators and using the closest production rate calibration, southern South America, which is statistically indistinguishable from calibrations elsewhere in the Southern Hemisphere (Kaplan et al., 2011). In more detail, consistent with the production rate calibration in Kaplan et al. (2011), we used version 2.2 with version 2.2.1 of the constants file (Balco et al., 2008) and a high-resolution version of the geomagnetic framework (Lifton et al., 2008). We show ages with the time dependent version of Stone/Lal scaling protocol scheme (Lm; Lal, 1991; Stone, 2000). For comparison, ages decrease using version 3 of the online calculator, by 1-5% (St/Lm), or 0 to >10% (LSD). Choice of scaling model and the version of the online calculator used do not affect our inferences and conclusions for two main reasons. First, and most important, we are aware of such uncertainties when discussing past glacier and climate changes. Second, analytical uncertainties (and moraine ages discussed) are typically >3%, and >5% for ages less than 1000 years (Table S2). To compare all ages around James Ross Island using consistent cosmogenic nuclide dating systematics, we recalculated results in prior studies (Johnson et al., 2011; Glasser et al., 2014; Nývlt et al., 2014).  $^{10}$ Be ages increase by >10% compared with those presented in prior works, mainly given use of an updated production rate calibration, as well as more recent dating systematics (Table S3). We report  $^{10}$ Be ages with  $1\sigma$  analytical uncertainty.

We carried out two approaches for sampling and dating, which we need to describe briefly, to understand our results. First, we sampled cobbles or boulders perched upon bedrock or ground moraine, and these ages are on materials left behind as ice ablated and receded. The second approach is to sample boulders or cobbles embedded in the tops of moraines that mark former glacier limits, as is common in the literature; <sup>10</sup>Be ages on lateral or frontal moraines denote when glaciers are in expanded positions relative to current glacier margins. We do not distinguish whether ages are likely to represent the end of a period of moraine building, possibly just prior to retreat, or near the end of moraine stabilization. In addition, we focus on general periods of glacier recession or advance, as this considers potential issues of relatively high scatter in glacier chronologies in high latitude environments, as discussed in more detail below.

#### 3. Results (Figs. 2-5; Tables S1-2)

#### 3.1. Long Island

Within a roughly  $100~\text{m}^2$  area, we sampled and measured six cobble-size samples of quartz-rich schist and granite lithologies (3 of each), which overlaid shattered metamorphic bedrock (Fig. 2A). These erratic cobbles remained as the large ice sheet retreated roughly westward back towards the Antarctic Peninsula, which is only  $\sim 3~\text{km}$  away. Two  $^{10}\text{Be}$  ages are  $10.6\pm0.6~\text{ka}$  and  $10.3\pm0.3~\text{ka}$ , and the other four ages range from  $8.2\pm0.3~\text{ka}$  to  $7.4\pm0.2~\text{ka}$ . The age distribution hence appears to be bimodal (Fig. 3), although we highlight the limited size of the dataset. We found no trend for age versus location or elevation. All samples are located between 91 and 95 m asl, within the error of the handheld GPS. All samples are cobble size and hence of a similar height above the underlying bedrock.

#### 3.2. Lagrelius Peninsula

We measured six granitic erratics (Fig. 2B) deposited (left behind) on a terrace-like feature that is in an area of  $\sim\!1~\rm km^2$ ; all six erratics are >30 m asl, well above recorded Holocene marine limits. We avoided areas of the terrace that had obvious solifluction, typical when the surface slopes reach more than  $\sim\!5^\circ$ , and depressions where snow persists even in summer. All six samples afford ages between 9.6±0.3 ka and 7.6±0.2 ka. There is a notable decrease of age towards lower elevations from  $\sim\!60$  m to 30 m asl, with one exception (8.6±0.2 ka) that deviates from a steady trend (Fig. 3C).

#### 3.3. Santa Martha Cove, Alpha Valley, and Dreadnought Point (Fig. 4)

All three sites are close to each other, along the west and southwest coast of Croft Bay (Fig. 1). The moraines at Alpha Glacier and Dreadnought Point are well-defined lateral landforms, whereas, the sampled deposit at Santa Martha is mapped as ground moraine although it is interpreted as a glacier limit (Fig. 4). All sampled moraines formed due to expansions of local terrestrial-based glaciers, after deglaciation. On Fig. 4, we show also two ages from Glasser et al. (2014) (-26 and -29),  $7.4\pm0.4$  ka and  $7.6\pm0.4$  ka, near Santa Martha Cove.

In more detail, on the south side of Santa Martha Cove five samples were embedded in ground moraine that is interpreted as marking a right lateral glacier position (Fig. 2D, 4).  $^{10}$ Be ages on igneous or metamorphic sample lithologies range from  $7.65\pm0.2$  ka to  $3.9\pm0.2$  ka, whereas, one age on a sandstone concretion is notably younger,  $1.7\pm0.1$  ka.

Farther south in the adjacent Alpha Glacier valley, we sampled a left lateral moraine; while one metamorphic sample affords an age of  $8.25\pm0.3$  ka, two sandstone concretions are much younger,  $2.8\pm0.1$  and  $2.1\pm0.1$  ka (Fig. 4). In addition, we measured four samples from sediments recently deposited near the present-day glacier front. Two of the four  $^{10}$ Be ages date two respective icecored frontal moraines ( $\sim$ 220 $\pm$ 20 and  $100\pm10$  yr). The two other samples are from emerging sediments accumulating near the left lateral ice edge/moraine contact: a sandstone cobble with  $^{10}$ Be concentrations equating to  $180\pm20$  years of exposure is from a supraglacial overthrusted debris band at the ice edge, while a  $420\pm20$  year exposed cobble is from till near the contact between the ice edge and lateral moraine.

At the southernmost site, Dreadnought Point, all four samples are inferred to be from a left lateral moraine formed by a glacier flowing north from inner Croft Bay (Fig. 4). The landform also could be part of a shared, interlobular, moraine from the confluence of two glaciers flowing northeast (Gamma Glacier) and north (Croft Glacier) (Fig. 1). Three ages on granite lithologies range from  $7.3\pm0.4$  to  $6.3\pm0.2$  ka, while one age on a sandstone clast is  $\sim 5.1\pm0.2$  ka. We note that the highest, unambiguous, wavewashed evidence observed at the site is  $\sim$ 8 m asl, about  $\sim$ 4 m below the lowest sample (Table S1). On the other hand, we also know that the maximum Holocene marine transgression recorded along western James Ross Island is between 20 and 15 m asl (Ingólfsson et al., 1992), consistent with the highest 15 m asl Holocene terrace recorded along northern part of the island (Hjort et al., 1997). We assume that a 20-15 ka marine terrace does not exist above the (local unambiguous)  $\sim$ 8 m marine limit, and hence above the Dreadnought Point samples, because the glacier (and/or ice shelf) still occupied inner Croft Bay (Fig. 4) until ~7ka, which formed the moraine (with granites from the local outcropping diamictons). Moreover, the Dreadnought Point moraine formed before marine limits of 8-5 m asl that subsequently shaped coastlines around 6 to 5 ka (Strelin et al., 2006). Alternatively, we note that all four ages may be minima because there possibly was a relatively brief period when they were shielded under water (and/or eroded out of moraine) during the transgression slightly before  $\sim$ 7 ka (Hjort et al., 1997)

#### 3.4. *Rhum area* (Fig. 5)

We measured 23 samples in the Rhum Cove and valley: (i) 7 samples (out of 23) date erratics left behind during glacier recession (Fig. 5, red color). Two of these 7 samples (11.9 $\pm$ 0.2 ka, 8.2±0.2 ka) were on top of a drumlinoid landform (Strelin and Malagnino, 1992) at the southwest corner of the fjord, and they are beyond all the dated moraines. The other 5 (out of 7) samples were on top of remnant ground (hummocky) moraine between right lateral moraine crests, and they appear to fall into two clusters; two boulders ages are in agreement with each other,  $\sim$ 5.2-5.1 ka, and three cobble ages are in agreement with each other, between  $\sim 3.5$ and 3.1 ka. (ii) 12 samples (out of 23) date lateral moraines on the sides of the Cove (Fig. 5, blue color). These 12 ages appear to cluster into three main groups, from ~4.8 ka to 4.5 ka, around 3.9 to 3.5 ka, and  $\sim$ 1.8-1.4 ka. (iii) Four cobble-sized samples date deposits relatively close to, or on, the present-day Rhum glacier front (Fig. 5); 2 of the 4 cobbles were located on frontal moraines  $(310\pm20 \text{ yr and } 230\pm10 \text{ yr})$ , 1 cobble was from the ice edge/innermost moraine contact area (100±10 yr), and 1 cobble was on top of sediment that recently emerged from the ice surface (120 $\pm$ 10 yr) (Fig. 2E). All four dated samples on Fig. 5 (bottom panel) are in morpho-stratigraphic order given uncertainties. On the other hand, we did note signs of ponding (e.g. water levels) and a potential outburst around the youngest sample (100±10 yr), which could explain, taken at face value, possibly a younger age compared with the 120±10 yr cobble on the recently emerged sediment. The decrease in glacier size shown by the four samples dated to <300 years has continued in recent decades, as a thicker than present Rhum Glacier was observed in 1979-1980 and 1987 (Strelin, unpublished observations).

#### 3.5. Seymour Island

We collected three samples from large granitic erratics located between  $\sim$ 200 and 210 m asl. They are located on till veneer and they were left behind as an extended ice sheet or local ice cap retreated during deglaciation. The samples afford ages of 9.3 ka $\pm$ 0.3, 5.3 $\pm$ 0.2, and 3.9 $\pm$ 0.2 ka. Johnson et al. (2011) also reported four ages from Seymour Island (Fig. 6A).

#### 4. Discussion

#### 4.1. Erratics left behind as ice ablated

For the timing of deglaciation and ice recession of the northern Antarctic Peninsula Ice Sheet, our findings build on previous studies on or near James Ross Island, including those involving <sup>10</sup>Be and <sup>14</sup>C dating (Fig. 6), and nearby offshore efforts using cores and multibeam-based ground morphology (e.g., Björck et al., 1996; Hjort et al., 1997; 1998; Pudsey and Evans, 2001; Brachfeld et al., 2003; Bentley et al., 2005; Pudsey et al., 2006; Strelin et al., 2006; Roberts et al., 2011; Balco et al., 2013; Minzoni et al., 2015; Jeong et al., 2018). The new <sup>10</sup>Be ages allow us to offer the following added insights into understanding Holocene deglaciation and ice recession in the inner fjords and onto land.

First, prior studies showed deglaciation reached the inner marine shelf and channels after  $\sim\!\!14$  ka (e.g., Brachfeld et al., 2003; Pudsey et al., 2006). By  $\sim\!\!11\text{-}9$  ka, widespread recession of the northern Antarctic Peninsula Ice Sheet occurred from Seymour Island to Cape Lachman, leading to the opening the Prince Gustav Channel, and exposing Long Island and western James Ross Island

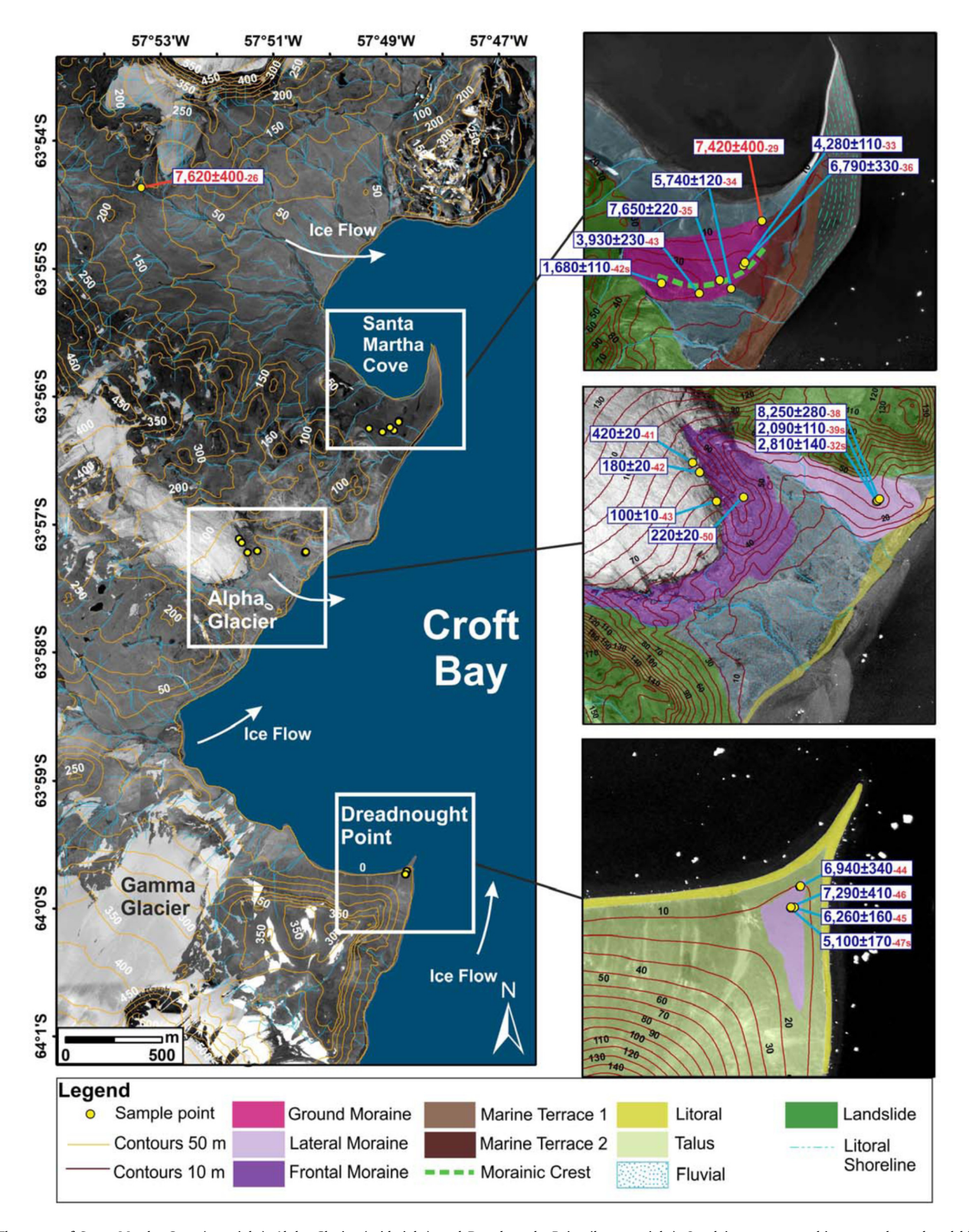


**Fig. 4.** The areas of Santa Martha Cove (top right), Alpha Glacier (mid right), and Dreadnought Point (bottom right). Overlain on geomorphic maps, the red and blue ages represent erratics left behind during recession and moraine samples, respectively, and follow color convention throughout the paper. The last two digits after each age (in red) is the sample label (Tables S1, S2). All <sup>10</sup>Be ages are measured on granites, except for four ages on sandstone concretions (*italicized*, 's' in red sample label), which are measured on cobble-sized samples and are younger than the granitoid ages (see text). Also shown are two ages from Glasser et al. (2014; -26 and -29), which were recalculated with same method systematics. Base maps are from the Czech Geological Survey (2009).

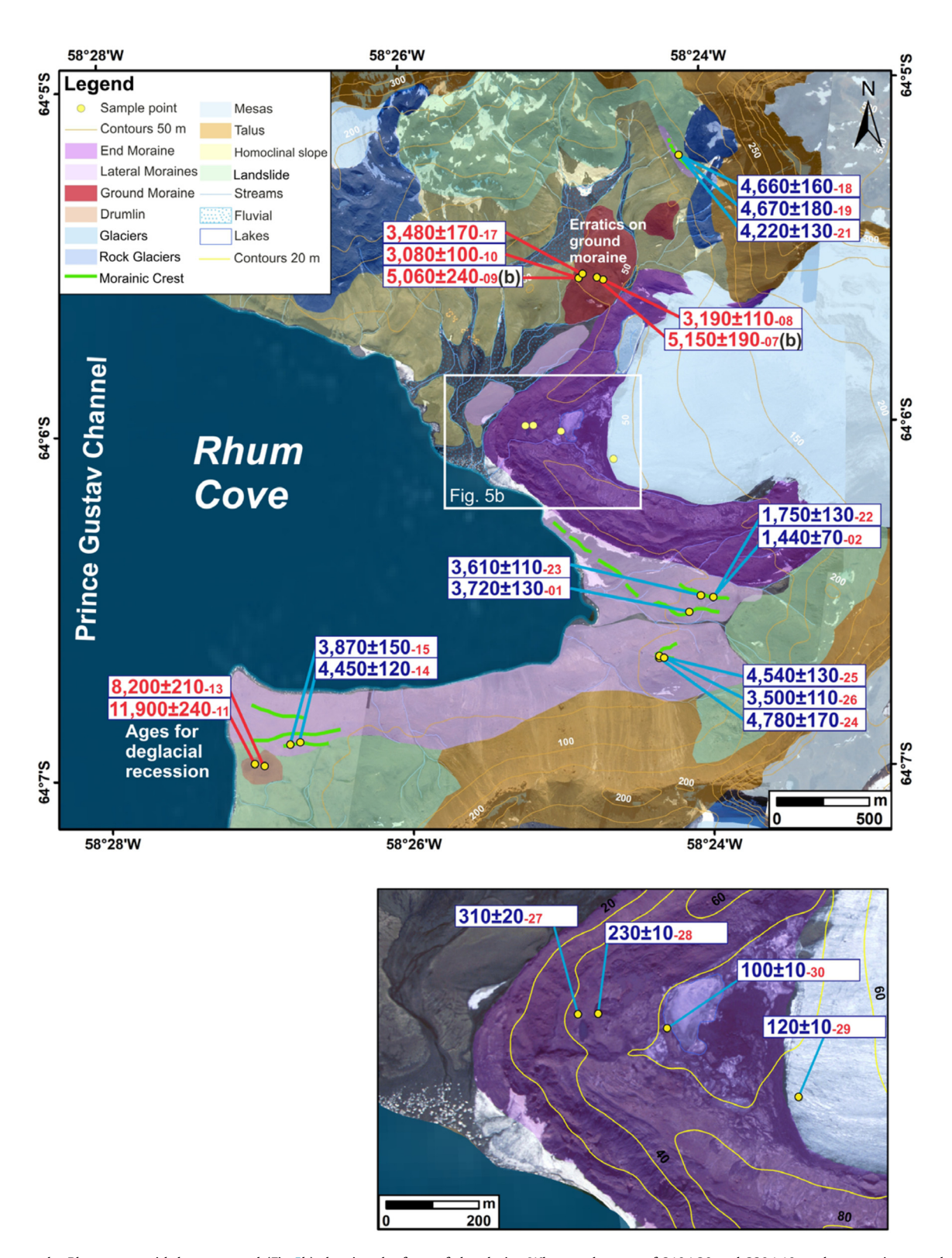


**Fig. 5.** Focus on the Rhum area, with bottom panel (Fig 5b) showing the front of the glacier. Whereas the ages of 310±20 and 230±10 yr date moraine samples, the two innermost ages (-30 and -29) are associated with debris bands sitting by the glacier front. We assume the two youngest ages reflect surface lowering over the last few decades (in agreement with Balco et al., 2013), causing emergence of the upward flowing till bands. Red and blue labels represent erratics left behind and lateral moraine samples, respectively, and follow convention throughout the paper. The last two digits refers to the sample label (Tables 1, S2). The 'b' after -07 and -09 labels represent samples are from a boulder (Table S1). Base images are aerial photos taken by Strelin in 2004 and 2006. Additional imagery with sample location shown in Supplementary Material (Fig. S1).

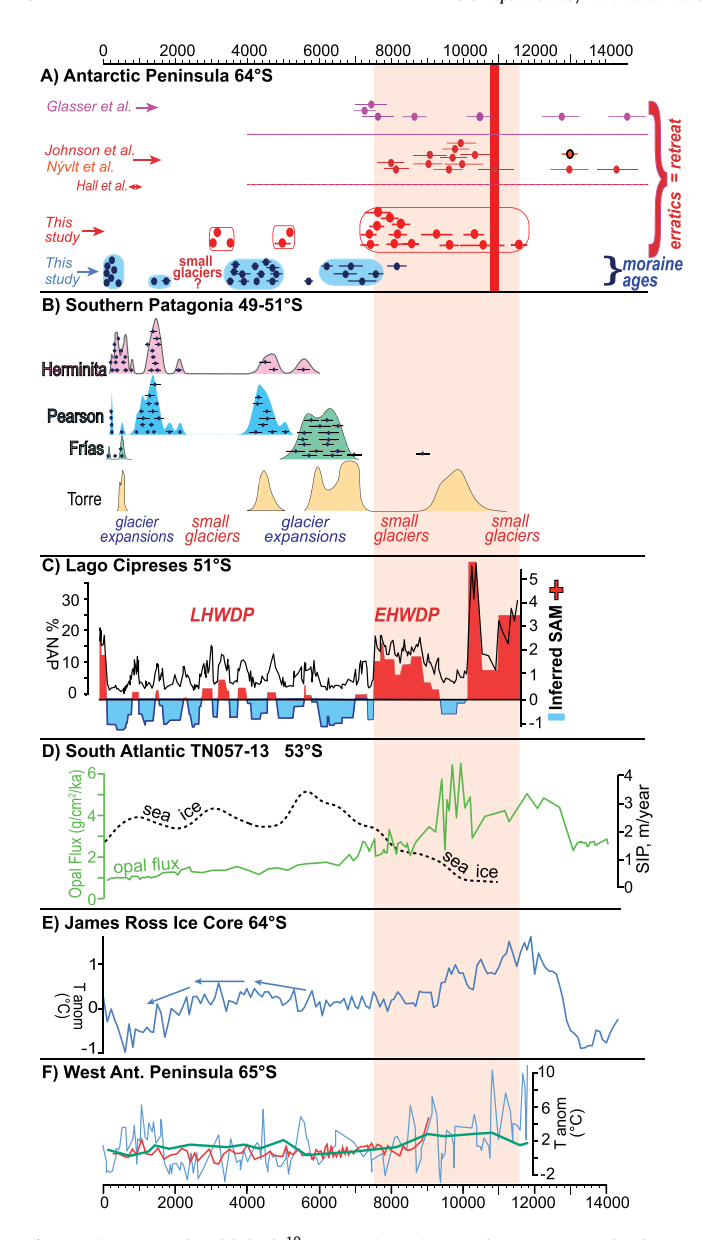


**Fig. 6. A).** New and published  $^{10}{
m Be}$  ages  $(\pm 1\sigma)$  around James Ross Island. Ages >14 ka and sandstone ages not shown (see text). Blue ovals highlight age ranges observed on the moraines. Also shown are the <sup>14</sup>C-dated moss (vertical red line) (Fig. 3), deposited as the ice sheet thinned (Ingólfsson et al., 1992), and a relatively warm period,  $\sim$ 1000-700 years ago, defined in Hall et al. (2010); **B)** We show  $^{10}$ Be ages  $(\pm 1\sigma)$  and summed probability distributions for 4 sites in southern Patagonia; the 'camel humps' reflect times of moraine formation (Kaplan et al., 2016; Reynhout et al., 2019), C) From Moreno et al. (2018), non-arboreal pollen (NAP, black) compared with the results of a regime shift detection algorithm applied to the data, and timing of the early Holocene and late Holocene warm dry periods (EHWDP and LH-WDP). Moreno et al. (2018) interpreted regime shift anomalies >0 (red filling) and <0 (blue filling) as positive and negative SAM-like states, respectively; D) From Mulvaney et al. (2012), temperature anomaly from Mont Haddington ice core: E) TEX86 derived sea surface temperature (SST) anomalies at ODP Site 1098 (blue is from Shevenell et al. (2011), green from Etourneau et al. (2013)); TEX<sub>86</sub> SST from nearby JPC-10 (red, Etourneau et al. (2013)); F) From Anderson et al. (2009), who interpreted opal flux as reflecting upwelling driven by the westerlies, and Divine et al. (2010). SIP=sea ice presence with 1000-year smoothing. Panels A to F show coherent climate signals for  ${\sim}15^{\circ}$  of latitude (Fig. 1). Vertical red band across panels A to F marks early Holocene warm period.

(Fig. 3) (Johnson et al., 2011; Glasser et al., 2014; Nývlt et al., 2014). The new  $^{10}$ Be ages indicate ice recession onto land at heads of bays and coves may have occurred slightly later by  $\sim$ 2-1 kyr, around 9-8 ka, specifically onto southwest and western James Ross and south of Herbert Sound into the central part of the island

(Fig. 3, 4). Our finding is consistent with Minzoni et al. (2015) who also concluded that ice recession reached the inner fjords by 8 to 7 ka.

Furthermore, given the ages become younger from  $\sim\!60~\mathrm{m}$  to 30 m asl (Fig. 3C) on the Lagrelius Peninsula, on the west side of James Ross Island, a net lowering of  $\sim\!30~\mathrm{m}$  of the ice surface from  $\sim\!9.5$  to 7.6 ka may be evident. Another possibility is that the difference in Lagrelius age with elevation relates to the movement and recession (thinning) of a 'relatively local' divide that separated ice flowing from both James Ross Island and from the Antarctic Peninsula, which channelized along the Prince Gustav channel, as postulated by Camerlenghi et al. (2001).

The 10Be ages from the top of Long Island, on samples between 95 and 91 m asl, form a bimodal distribution. Additional data are needed to evaluate the bimodality. Perhaps the two older ages (>10 ka) indicate the deglacial timing, and the younger sample ages (<10 ka) are minima (due to frost disturbance?), or a short (~3 km) readvance from the Antarctic Peninsula to Long Island deposited the 8-7 ka cobbles and did not disturb the two older samples, which contain some inherited <sup>10</sup>Be. For now, we infer that the oldest ages ( $\sim$ 10.6 and 10.3 ka) likely reflect recession of the Antarctic Peninsula Ice Sheet for the following reasons. First, an age around >10 ka agrees with the inference of Pudsey et al. (2006) for the decoupling of ice in the southern part of the Prince Gustav Channel, between 10.9 and 10.7 cal ka BP. Second, the older Long Island <sup>10</sup>Be ages are consistent with the ages for ice recession from the top (50 to 60 m asl) of a drumlin on the southeast side of Rhum Bay (Fig. 5). Ice recession across Long Island around or slightly before 10 ka is also consistent with the  $^{\bar{14}}\text{C-dated}$  moss age on Lachman Peninsula (Figs. 3, 6A). That is, Ingólfsson et al. (1992) obtained a  $^{14}\text{C}$  age of  $9525\pm65$  (10,  $810~\pm160$  cal yr BP, Oxcal 4.3) on terrestrial fresh water moss growing in an ice-marginal lake along Lachman Peninsula. We infer this <sup>14</sup>C age, on an insitu terrestrial macrofossil, to represent a key deglacial constraint. The lacustrine moss indicates that ice had thinned enough for an ice marginal lake to exist along the west (left) lateral side of the receding ice tongue in Herbert Sound, but the glacial ice dam still had to exist over an area that is now filled by the ocean (Herbert Sound and Croft Bay).

We note the  $^{10}$ Be data in Nývlt et al. (2014) imply a slightly earlier timing for deglaciation around northwestern James Ross Island, as all ages are >13 ka, based on up-to-date  $^{10}$ Be dating systematics. As mentioned in Nývlt et al. (2014), one possibility is their younger ages (assuming older ages have inheritance) represent earlier ice thinning in phase with regional warming. For example, the  $^{14}$ C-dated moss of 10,810 cal yr BP (Ingólfsson et al., 1992) is  $\sim$ 12 m asl in elevation, whereas the  $^{10}$ Be-dated boulders in Nývlt et al. (2014) are higher,  $\sim$ 40-50 m asl.

#### 4.2. Moraine dates and times of expanded glaciers

We provide a new  $^{10}$ Be-based chronology of Holocene glacier changes on James Ross Island, including the first ages spanning the last few hundred years (Figs. 4, 5, 6A). A key take away is that there is a distinct difference in timing between ages reflecting general ice recession across the area prior to  $\sim$ 8-7 ka and moraine building events after (Fig. 6A). Collectively, considering all sites (Tables S1, S2), coherent moraine ages cluster between  $\sim$ 8-7 and  $\sim$ 6-5 ka, 5 and 3.5 ka,  $\sim$ 1.5 ka, and over the last 300 years (Figs. 4, 5, 6A). The oldest moraine age (only one age),  $\sim$ 8 ka, is at the entrance to the Alpha valley (Fig. 4). The Rhum valley has the most comprehensive record (Fig. 5). Only one moraine (i.e., a former glacier limit) exists at Dreadnought Point (Fig. 4), which affords three relatively coherent middle Holocene  $^{10}$ Be ages of  $\sim$ 7-6 ka. At Santa Martha, boulders on ground moraine afford the most scattered distribution of any single morainic landform (see Fig. S1

in Supplementary Material). Moreover, at Santa Martha no glacier has existed since the middle Holocene and thus younger moraines there did not form. We also point out that we have only dated a few moraines in this study and our overall record is likely incomplete.

The spread in individual moraine age distributions beyond  $2\sigma$  uncertainty, specifically at the Santa Martha site (Figs. 4, S1), could reflect several possibilities. First, ice margins may have reached the same position more than once. Second, some of the ages are maxima due to nuclide inheritance. Third, some of the ages are minima due to snow cover and/or postglacial frost shattering processes (e.g., erosion). Or, there was a prolonged period of ice cored moraine stabilization.

To evaluate the second possibility, whether inherited nuclide concentrations are a problem in the study area, we measured recently emerged cobbles at two sites. In the front of the Rhum Glacier, all four <sup>10</sup>Be ages are in stratigraphic agreement, including the 120±10 yr cobble from a debris band on the ice near its front (Fig. 5B). At the Alpha Glacier, along the left lateral, one age on a cobble coming out of the ice recently and one age at the ice/moraine contact are older than the frontal moraine ages. Slight differences between the left lateral and frontal ages perhaps provide insight into possible processes related to the subpolar thermal regime (Chinn and Dillon, 1987; Chinn, 1991; Strelin and Sone, 1998). As the glacier front is likely frozen to its bed, this obstruction of flow causes debris to rise to the surface along shear zones. For the sake of argument, if the regelation front migrated up-valley over the last few hundred years, due to climate change, then debris will be extruded that originated from higher levels of the basal glacier zone, and different surface sediment accumulations near the front may contain cobbles with varying ages. Regardless of how cobbles came out of the surface, our findings indicate there is minimal inheritance in late Holocene moraine samples on James Ross Island, indicating an opportunity for additional dating.

Regarding the third possibility, geomorphic processes reduced some apparent ages, we tried to avoid slopes or obvious signs of periglacial processes. However, many samples are relatively short such as the cobbles (Table S2), which could have had some degree of snow cover for parts of the year. At Lagrelius Peninsula and other sites, we found no obvious relation between boulder age and height above ground (Table S2), as might be expected with snow cover. The sandstone samples always afford younger ages than the metamorphic and igneous materials. The sandstones may be less resistant to weathering because internal layering makes them relatively more susceptible to periglacial processes (frost shattering, frost heaving); two of the cobbles were concretion-like with possible evidence of minor spalling. In addition, two new Seymour Island <sup>10</sup>Be ages (Fig. 1) are much younger than the deglacial ages including those in Johnson et al. (2011). We cannot explain why two new Seymour 10 Be ages are so young, except perhaps a small ice cap or snow cover persisted for much of the Holocene (such as currently exist on Snow Hill Island) at the sites where the new samples are from on the relatively high plateau of the southwest

Given the apparent lack of inheritance in samples from glacier limits of the last few hundred years, we assume the age scatter on moraines is mainly due to geomorphic processes that act to minimize ages. This effect may be most pronounced in the Santa Martha area (Figs. 4, S1), where perhaps the ground moraine is also not a distinct glacier limit as we mapped (Fig. 4), but represents a compound deposit of more than one advance. Regardless, such scatter does not affect our main inferences, as we recognize precise (sub-century or century) one-to-one correlations likely are not yet possible between the <sup>10</sup>Be dated glacier record and other proxies (Fig. 6).

The results are in agreement with prior work on James Ross Island that defined local glacier expansions at 7.3 to 7.1 ka, 5.3 to 4.8 ka, shortly after 4.1 or after 3 ka, between 2.7 and 2 ka, 1.2 ka to 950 yr, and during the last  $300^{-14}$ C yr B.P (e.g., Zale and Karlen, 1989; cf., Clapperton and Sugden, 1988; Strelin et al., 2006). Nearby, Balco et al. (2013) and Jeong et al. (2018) inferred grounding line and ice shelf readvances after  $\sim$ 2 ka. Also, Strelin et al. (2006) studied ice cored moraines and rock glaciers that they inferred correspond to glacier advances over the last millennium. In Herbert Sound, Minzoni et al. (2015) observed glacier activity especially after  $\sim$ 2.5 ka, although evidence of earlier activity is not clear.

#### 4.3. Antarctic Peninsula-Southern Patagonia-South Atlantic

To place the new results in a broader hemispheric context, we compare the findings with  $^{10}$ Be-dated glacier and  $^{14}$ C-dated pale-oecologic records in southern Patagonia (Fig. 6A-C), and with marine and ice cores around the southern South Atlantic and northern Antarctic Peninsula (Fig. 6D-F). In the early Holocene, both the Antarctic Peninsula (e.g., Bentley et al., 2005) and southern Patagonia experienced warm conditions, except perhaps from  $\sim 10$  to 9.5 ka. Around James Ross Island, deglaciation occurred and local glaciers subsequently retreated towards embayment heads and onto land. In Patagonia, during the early Holocene glaciers were typically similar in extent as today (e.g., Strelin et al., 2014; Menounos et al., 2013). Moreno et al. (2018) defined the Early Holocene Warm Dry Period from  $\sim 10.5$  to 7.5 ka (Fig. 6C).

The early Holocene warm interval ended evidently by  $\sim$ 8-7 ka, and thereafter glacier expansions repeatedly occurred in both Patagonia and the Antarctic Peninsula (Figs. 4–6). Precise one-to-one correlations at the subcentury and century level may be tenuous given the limited number of moraine ages on James Ross (and scatter discussed above). Periods that were generally favorable for glaciers expanding on both sides of the Drake Passage occurred between  $\sim$ 7-6 ka and 5-4 ka, and after 3 ka (Fig. 6). Our findings are in agreement with prior terrestrial studies in the James Ross area (e.g., Ingólfsson et al., 1992; Hjort et al., 1997; 1998, Strelin et al., 2006). For example, an ice core at the summit of Haddington Ice Cap reveals pronounced Holocene warmth until  $\sim$ 8 ka (Fig. 6E; Mulvaney et al., 2012), consistent with wider geographic findings in Masson et al. (2000).

After the early Holocene, warm intervals occurred on either side of the Drake Passage, and there are general gaps in moraine building events from  $\sim$ 4 to 2.5 ka and from  $\sim$ 1000 to 700 years ago (Fig. 6A, B). Regarding the former period, from  $\sim$ 5 to 3 ka has long been identified as a time of general warmth around James Ross Island, as well as elsewhere in Antarctica, including reduced ice and absence of local ice shelves (e.g., Hjort et al., 1998; Pudsey and Evans, 2001; Brachfeld et al., 2003; Strelin et al., 2006; Balco et al., 2013; Jeong et al., 2018). Björck et al. (1996) defined the interval from  $\sim$ 4.8 to 3 ka as the Holocene climatic optimum, a period of relative warmth when glaciers were receded. More recently, Minzoni et al. (2015) described marine environmental conditions in Herbert Sound and Croft Bay, near the St. Martha site (Fig. 1) as occurring during a mid-late Holocene hypsithermal,  $\sim$ 5.5 to 3 ka. On the other hand, evidence presented here such as in the Rhum valley (Fig. 5) and in prior studies (e.g., near Lagrelius Peninsula; Strelin et al., 2006), may imply that climatic conditions were not uniformly warm during the 5 to 3 ka interval. We propose that either the precise start of the 5-3 ka general warm event needs to be revised slightly (especially given bulk 14C dating or need for marine reservoir corrections), or the  $\sim$ 2 kyr interval was a period of both warm and (brief) cold periods. The glacier records shown in Fig. 6 may imply that the warmest or most sustained conditions of the (mid-late) Holocene climatic optimum were between ~4 and

 $\sim$ 3 ka, peaking closer to the latter. For comparison, the James Ross Island ice core data (Fig. 6E) exhibit the highest temperatures from  $\sim$ 4 to 3 ka. In Patagonia, Moreno et al. (2018) referred to the interval from  $\sim$ 4 to  $\sim$ 3 as the Late Holocene Warm Dry period (Fig. 6. LHWDP).

Our findings are consistent with broad trends observed on the west side of the Antarctic Peninsula. Marine records reveal marked early Holocene warmth (Shevenell et al., 2011; Etourneau et al., 2013; Pike et al., 2013) (Fig. 6F); Etourneau et al. (2013) also observed decreased seasonal sea ice presence as indicated by open ocean and warm-affinity diatoms. Thereafter, cooling occurred through the middle Holocene and increased seasonal sea ice presence. Over the last few thousand years, the western Antarctic Peninsula may have experienced a longer annual sea ice duration but relatively warm but brief summers (Etourneau et al., 2013). For comparison, in the late Holocene glacier advances on James Ross Island and in Patagonia exhibit a general pattern of decreasing size (Figs. 4, 5). Moreover, on Anvers Island, Hall et al. (2010) noted a prominent warm period from 970–700 yr ago (Fig. 6A), which Bentley et al. (2009) also discussed.

Thus, we conclude that during the early Holocene diverse records collectively imply that a broad spatial swath of warmth existed most of the time from middle latitude South America and the Subantarctic circumpolar region across to the Antarctic Peninsula (Fig. 6). During this time, in the southern South Atlantic near the Subantarctic front (Fig. 6D), Anderson et al. (2009) inferred high rates of upwelling due to a poleward expansion of the westerlies, and annual sea ice presence was at a minimum (Divine et al., 2010). We infer that a poleward expansion of the band of (relatively) stronger westerlies during the early Holocene explains the findings shown in Fig. 6A to F. Toggweiler and Russell (2008) argued that a general characteristic of warm climates, such as the present interglacial, is a poleward shift and linked intensification of the westerlies, even if the winds tend to weaken at mid-latitudes (Moreno et al., 2018). Subsequently, for the rest of the Holocene sea ice was more persistent, perhaps achieving maximum extents around 6-5 ka (Divine et al., 2010; Etourneau et al., 2013).

In addition, we infer overall glacier-climate behavior around the Antarctic Peninsula is congruent with reconstructed Southern Annular Mode (SAM)-like conditions at the multi-century and millennial timescales (Fig. 6C; Moreno et al., 2018). During the Early Holocene, SAM-like conditions were persistently positive and moraines are generally lacking in southern South America and the James Ross region (Fig. 6A, B); except from  $\sim$ 10 to 9.5 ka when SAM-like conditions briefly turned persistently negative (Fig. 6B). After 8-7 to ~5 ka, persistent negative SAM-like centennial conditions are reconstructed in southern Patagonia (Moreno et al., 2018) and glacier expansions are documented on both sides of the Drake Passage (Fig. 6). From ~4 to 2.5 ka, positive SAM-like conditions typically occurred (Fig. 6A, C) and temporal gaps between moraine-building events are common on both sides of the Drake Passage. After 3 ka, SAM-like conditions were persistently negative and glaciers likewise expanded on both sides of the Drake Passage (Fig. 5, 6C) (cf., Balco et al., 2013).

Over the instrumental time period negative SAM characteristically includes increased frontogenetic conditions in all seasons as far north as central South America, as well as a large region over the South Atlantic Ocean, as the subtropical jet is strengthened and it drifts equatorward along with Subantarctic climates (Carvalho et al., 2005; Reboita et al., 2009). Likewise, we infer such characteristics were pervasive in the past during persistent negative SAM-like conditions. Positive SAM phases characteristically involve the opposite behavior of negative SAM, such as poleward expansion of the band of stronger westerlies (Moreno et al., 2018).

Further investigation is needed to improve the comparison at centennial and sub-centennial timescales between the eastern and western Antarctic Peninsula and with southernmost South America. For example, researchers infer that there is a strong influence of ENSO and possibly the Antarctic Dipole on Antarctic Peninsula climates, especially on the west side over recent decades and millennia (Shevenell et al., 2011; Etourneau et al., 2013; Pike et al., 2013; Yuan et al., 2018). We infer at least broad patterns (e.g., millennial?) of glacier behavior are coherent across the middle-high latitudes (Fig. 6) of southern South America and the eastern Antarctic Peninsula.

#### 5. Summary and conclusions

We obtained a 10 Be dataset for James Ross Island and nearby Long Island and Seymour Islands. While our study builds on existing data for the deglaciation, we present a new 10Be-based chronology of Holocene local glacier changes. In the early Holocene, widespread ice recession or reduced glacier coverage existed most of the time from southern South America to the northern Antarctic Peninsula. Early Holocene warmth lasted until about ~8 ka, and it was a period of reduced sea ice in the South Atlantic (Fig. 6), and was widespread across other sectors of Antarctica (e.g., Masson et al., 2000). After  $\sim$ 8 ka, cooler conditions generally existed over the remainder of the Holocene, and glaciers repeatedly expanded. Advances around the northeastern Antarctic Peninsula occurred at least from 7.5 to 7 ka,  $\sim$ 5-4 ka (Fig. 5 and in Strelin et al., 2006), perhaps at times between 3.9 and 3.6 ka and just after 3 ka (Strelin et al., 2006), between  $\sim$ 2.4 and  $\sim$ 1 ka, and over the last few centuries. Since deglaciation, the largest glacier extents occurred in the middle Holocene,  $\sim$ 7-4 ka. The advances of the last few centuries on James Ross Island (and in Patagonia) overlap in time with the Little Ice Age interval in Europe, although the exact relations still need to be determined. We also infer the general cooling after  $\sim$ 8-7 ka could have played an important role in regrowth of ice around the southern Weddell Sea (cf., Kingslake et al., 2018).

Even though middle to late Holocene conditions were generally cool, notable warm interruptions occurred. The most pronounced was the Holocene climate optimum, previously defined from  $\sim$ 5 to  $\sim$ 3 ka around the Antarctic Peninsula. We infer that climate conditions were not constant from 5 to 3 ka and that peak warmth may have occurred between  $\sim$ 4 and  $\sim$ 3 ka around the eastern Antarctic Peninsula and in Patagonia.

To conclude, paleo records from the middle (Subantarctic) to high latitudes reveal coherent climate shifts over  $\sim 15^{\circ}$  of latitude, and glaciers tracked Westerly and polar vortex behavior and perhaps SAM-like conditions. Reduced glacier extents occur when there is less extensive South Atlantic and high-latitude sea ice and the westerlies expand and polar vortex contracts poleward, such as during the Holocene prior to  $\sim$  8 ka. The opposite glacier behavior occurs when sea ice is more extensive, the westerlies and the polar vortex (and subtropical jet; Carvalho et al., 2005) are more focused or expand equatorward, and SAM-like negative states are persistent at the century scale. If glaciers, and by implication ice shelves, are particularly sensitive to positive SAM-like conditions, reduced sea ice extent, and poleward expansion of the westerlies, then this has an important implication for future cryospheric behavior. SAM has been persistently positive in recent decades and modeling simulations foretell a consistent pattern in the near future (Abram et al., 2014).

#### **Declaration of competing interest**

The authors declare that they have no known competing financial interests or personal relationships that could have appeared to influence the work reported in this paper.

#### Acknowledgements

We want to express our gratitude to the personnel of the Instituto Antártico Argentino (IAA), Dirección Nacional del Antártico (DNA), and Fuerza Aérea Argentina, for their logistic support. We thank Jeremy Frisch and Jean Hanley for laboratory assistance. We thank Greg Balco, Matias Barrionuevo, Patricio Moreno (especially for important suggestion for Fig. 6C), Xiaojun Yuan, and Julia Gottschalk for discussion and anonymous Reviewers who helped greatly to strengthen the manuscript. We acknowledge support by PICTA, 2011–0102, Instituto Antártico Argentino-SECyT, "Geomorfología y Geología Glaciar del Archipiélago James Ross e Islas Shetland del Sur, Sector Norte de la Península Antártica", granted to J.A.S., and National Science Foundation PLR-11-42002 to MK, JS, and GW. This is LDEO contribution 8375.

#### Appendix A. Supplementary material

Supplementary material related to this article can be found online at https://doi.org/10.1016/j.epsl.2020.116077.

#### References

- Abram, N.J., Mulvaney, R., Vimeuz, F., Phipps, S.J., Turner, J., England, M.H., 2014. Evolution of the southern annular mode during the past millennium. Nat. Climate Change 4, 564–569.
- Anderson, R.F., Ali, S., Bradtmiller, L.I., Nielsen, S.H.H., Fleisher, M.Q., Anderson, B.E., Burckle, L.H., 2009. Wind-driven upwelling in the Southern Ocean and the deglacial rise in atmospheric CO<sub>2</sub>. Science 323, 1443–1448.
- Balco, G., Stone, J., Lifton, N., Dunai, T., 2008. A simple, internally consistent, and easily accessible means of calculating surface exposure ages and erosion rates from Be-10 and Al-26 measurements. Quat. Geochronol. 3, 174–195.
- Balco, G., Schaefer, J.M., LARISSA group, 2013. Exposure-age record of Holocene ice sheet and ice shelf change in the northeast Antarctic Peninsula. Quat. Sci. Rev. 59, 101–111.
- Bentley, M.J., Hodgson, D.A., Sugden, D.E., Roberts, S.J., Smith, J.A., Leng, M.J., Bryant, C., 2005. Early Holocene retreat of the George VI ice shelf, Antarctic Peninsula. Geology 33, 173–176.
- Bentley, M.J., Hodgson, D.A., Smith, J.A., Ó Cofaigh, C., Domack, E.W., Larter, R.D., Roberts, S.J., Brachfeld, S., Leventer, A., Hjort, C., Hillenbrand, C-D., Evans, J., 2009. Mechanisms of Holocene paleoenvironmental change in the Antarctic Peninsula region. Holocene 19, 51–69.
- Björck, S., Olsson, S., Ellis-Evans, S., Håkansson, H., Humlun, O., Lirio, J.M., 1996. Late Holocene paleoclimatic records from lake sediments on James Ross Island, Antarctica. Palaeogeogr. Palaeoclimatol. Palaeoecol. 121, 195–220.
- Brachfeld, S., Domack, E., Kissel, C., Laj, C., Leventer, A., Ishman, S., Gilbert, R., Camerlenghi, A., Eglinton, L.B., 2003. Holocene history of the Larsen-a ice shelf constrained by geomagnetic paleointensity dating. Geology 31, 749–752.
- Camerlenghi, A., Domack, E., Rebesco, M., Gilbert, R., Ishman, S., Leventer, A., Brachfeld, S., Drake, A., 2001. Glacial morphology and post-glacial contourites in northern Prince Gustav Channel (NW Weddell Sea Antarctica). Mar. Geophys. Res. 22, 417–443.
- Carvalho, L.M., Jones, C., Ambrizzi, T., 2005. Opposite phases of the Antarctic oscillation and relationships with intraseasonal to interannual activity in the tropics during the austral summer. J. Climate 18, 702–718.
- Chinn, T.J., 1991. Polar glacier margin and debris features. Mem. Soc. Geol. Ital. 46, 25–44.
- Chinn, T.J., Dillon, A., 1987. Observations on a debris-covered glacier "Whiskey Glacier", James Ross Island, Antarctic Peninsula, Antarctica. J. Glaciol. 33, 300–310.
- Clapperton, C., Sugden, D., 1988. Holocene glacier fluctuation in South America and Antarctica. Quat. Sci. Rev. 7, 185–198.
- Czech Geological Survery, 2009. In: Nývlt, D., Šerák (Eds.), James Ross Island. Geological Map of the Northern Part. 1:25 000. Czech Geological Survey and GEODIS BRNO Ltd., Brno, Czech Replublic.
- Davies, B.J., Hambrey, M.J., Smellie, J.S., Carrivick, J.L., Glasser, N.F., 2012. Antarctic Peninsula Ice Sheet evolution during the Cenozoic Era. Quat. Sci. Rev. 31, 30–66.
- Davies, B.J., Golledge, N.R., Glasser, N.F., Carrivick, J.L., Ligtenberg, S.R.M., Barrand, N.E., van den Broeke, M.R., Hambrey, M.J., Smellie, J.L., 2014. Modelled glacier response to centennial temperature and precipitation trends on the Antarctic Peninsula. Nat. Climate Change 4, 993–998.
- Divine, D.V., Koc, N., Isaksson, E., Nielsen, S., Crosta, X., Godtliebsen, F., 2010. Holocene Antarctic climate variability from ice and marine sediment cores: insights on ocean-atmosphere interaction. Quat. Sci. Rev. 29, 303–312.

- Etourneau, J., Collins, L.G., Willmott, V., Kim, J.-H., Barbara, L., Leventer, A., Schouten, S., Sinninghe Damsté, J.S., Bianchini, A., Klein, V., Crosta, X., Massé, G., 2013. Holocene climate variations in the western Antarctic Peninsula: evidence for sea ice extent predominantly controlled by changes in insolation and ENSO variability. Clim. Past 9, 1431–1446.
- Glasser, N.F., Davies, B.J., Carrivick, J.L., Rodés, A., Hambrey, M.J., Smellie, J.L., Domack, E., 2014. Ice-stream initiation, duration and thinning on James Ross Island, northern Antarctic Peninsula. Quat. Sci. Rev., 78–88.
- Hall, B., Koffman, T., Denton, G., 2010. Reduced ice extent on the western Antarctic Peninsula at 700-970 cal yr B.P. Geology 38, 635-638.
- Hjort, C., Ingólffson, Ó., Möller, P., Lirio, J.M., 1997. Holocene glacial history and sea-level changes on James Ross Island, Antarctic Peninsula. J. Quat. Sci. 12, 259–273
- Hjort, C., Bjorck, S., Ingólffson, Ó., Möller, P., 1998. Holocene deglaciation and climate history of the northern Antarctic Peninsula region: a discussion of correlations between the southern and northern hemispheres. Ann. Glaciol. 27, 110–112.
- Ingólfsson, Ó., Hjort, C., Björck, S., Lewis-Smith, R.I., 1992. Late Pleistocene and Holocene glacial history of James Ross Island, Antarctic Peninsula. Boreas 21, 209–222.
- Jeong, A., Lee, J.I., Seong, Y.B., Balco, G., Yoo, K.-C., Yoon, H.O., Domack, E., Rhee, H.H., Yu, B.Y., 2018. Late quaternary deglacial history across the Larsen B embayment, Antarctica. Quat. Sci. Rev. 189, 134–148.
- Johnson, J.S., Bentley, M.J., Roberts, S.J., Binney, S.A., Freeman T, S.P.H., 2011. Holocene deglacial history of the North East Antarctic Peninsula a review and new chronological constraints. Quat. Sci. Rev. 30, 3791–3802.
- Kaplan, M.R., Strelin, J.A., Schaefer, J.M., Denton, G.H., Finkel, R.C., Schwartz, R., Putnam, A.E., Vandergoes, M.J., Goehring, B.M., Travis, S.G., 2011. In-situ cosmogenic <sup>10</sup>Be production rate at Lago Argentino, Patagonia: implications for late-glacial climate chronology. Earth Planet. Sci. Lett. 309, 21–32.
- Kaplan, M.R., Schaefer, J.M., Strelin, J.A., Denton, G.H., Anderson, R.F., Vandergoes, M.J., Finkel, R.C., Schwartz, R., Travis, S.G., Garcia, J.L., Martini, M.A., Nielsen, S.H.H., 2016. Patagonian and southern South Atlantic view of Holocene climate. Quat. Sci. Rev. 141, 112–125.
- Kingslake, J., Scherer, R.P., Albrecht, T., Coenen, J., Powell, R.D., Reese, R., Stansell, N.D., Tulaczyk, S., Wearing, M.G., Whitehouse, P.L., 2018. Extensive retreat and re-advance of the West Antarctic ice sheet during the Holocene. Nature 558, 430–434.
- Lal, D., 1991. Cosmic-ray labeling of erosion surfaces in-situ nuclide production rates and erosion models. Earth Planet. Sci. Lett. 104, 424–439.
- Lifton, N., Smart, D., Shea, M., 2008. Scaling time-integrated in situ cosmogenic nuclide production rates using a continuous geomagnetic model. Earth Planet. Sci. Lett. 268, 190–201.
- Masson, V., Vimeux, F., Jouzel, J., Morgan, V., Delmotte, M., Ciais, P., Hammer, C., Johnsen, S., Lipenkov, V.Y., Mosley-Thompson, E., Petit, J.-R., Steig, E., Stievenard, M., Vaikmae, R., 2000. Holocene climate variability in Antarctica based on 11 ice cores isotopic records. Quat. Res. 54, 348–358.
- Menounos, B., Clague, J.J., Osborn, G., Davis, P.T., Ponce, F., Goehring, B.M., Maurer, M., Rabassa, J., Coronato, A., Marr, R., 2013. Latest Pleistocene and Holocene glacier fluctuations in southernmost Tierra del Fuego, Argentina. Quat. Sci. Rev. 77, 70–79.
- Minzoni, R.T., Anderson, J.B., Fernandez-Vasquez, R.A., Wellner, J.S., 2015. Marine record of Holocene climate, ocean, and cryosphere interactions: Herbert sound, James Ross Island, Antarctica. Quat. Sci. Rev. 129, 239–259.
- Moreno, P.I., Vilanova, Villa-Martínez, R., Dunbar, R.B., Mucciarone, D.A., Kaplan, M.R., Garreaud, R.D., Rojas, M., De Pol-Holz, R., Lambert, F., 2018. Onset and evolution of southern annular mode-like changes at centennial timescale. Sci. Rep. 8, 3458.
- Moy, C.M., Moreno, P.I., Dunbar, R.B., Francois, J-P., Kaplan, M.R., Villalba, R., Haberzettle, T., 2009. Climate change in southern South America during the last two millennia. In: Vimeux, F., Sylvestre, F., Khodri, M. (Eds.), Past Climate Variability from the Last Glacial Maximum to the Holocene in South America and Surrounding Regions. In: Springer-Developments in Paleoenvironmental Research Series (DPER), pp. 353–393.
- Mulvaney, R., Abram, N.J., Hindmarsh, R.C.A., Arrowsmith, C., Fleet, L., Triest, J., Sime, L.C., Alemany, O., Foord, S., 2012. Recent Antarctic Peninsula warming relative to Holocene climate and ice-shelf history. Nature 89, 141–144.
- Nývlt, D., Braucher, R., Engel, Z., Mlčoch, B., 2014. Timing of the northern Prince Gustav ice stream retreat and the deglaciation of northern James Ross Island, Antarctic Peninsula during the last glacial-interglacial transition. Quat. Res. 82, 441-449
- O'Cofaigh, C., Davies, B.J., Livingstone, S.J., Smith, J.A., Johnson, J.S., Hocking, E.P., Hodgson, D.A., Anderson, J.B., Bentley, M.J., Canals, M., Domack, E., Dowdeswell, J.A., Evans, J., Glasser, N.F., Hillenbrand, C.D., Larter, R.D., Roberts, S.J., Simms, A.R., 2014. Reconstruction of ice-sheet changes in the Antarctic Peninsula since the last glacial maximum. Quat. Sci. Rev. 100, 87.
- Pike, J., Swann, G.E.A., Leng, M.J., Snelling, A.M., 2013. Glacial discharge along the West Antarctic Peninsula during the Holocene. Nat. Geosci. 6, 199–202.
- Pudsey, C.J., Evans, J., 2001. First survey of Antarctic sub-ice shelf sediments reveals mid-Holocene ice shelf retreat. Geology 29, 787–790.

- Pudsey, C.J., Murray, J.W., Appleby, P., Evans, J., 2006. Ice shelf history from petrographic and foraminiferal evidence, northeast Antarctic Peninsula. Quat. Sci. Rev. 25, 2357–2379.
- Reboita, M.S., Ambrizzi, T., da Rocha, R.F., 2009. Relationship between the southern annular mode and southern hemisphere atmospheric systems. Rev. Bras. Meteorol. 24, 48–55.
- Reynhout, S.A., Sagredo, E.A., Kaplan, M.R., Aravena, J.C., Martini, M.A., Moreno, P.I., Rojas, M., Schwartz, R., Schaefer, J.M., 2019. Patagonian glacier fluctuations modulated by local insolation and paced by Southern Annular Mode-like changes during the Holocene. Quat. Sci. Rev. 220, 178–187.
- Roberts, S.J., Hodgson, D.A., Sterken, M., Verleyen, E., Vyverman, W., Sabbe, K., Balbo, A., Bentley, M.J., Whitehouse, P.L., 2011. Geological constraints on glacio-isostatic adjustment models of relative sea-level change during deglaciation of Prince Gustav Channel, Antarctic Peninsula. Quat. Sci. Rev. 30, 3603–3617.
- Schaefer, J.M., Denton, G.D., Kaplan, M.R., Putnam, A., Finkel, R.C., Barrell, D.J.A., Andersen, B.G., Schwartz, R., Mackintosh, A., Chinn, T., Schlüchter, C., 2009. Highfrequency Holocene glacier fluctuations in New Zealand differ from the northern signature. Science 324, 622–625.
- Shevenell, A.E., Ingalls, A.E., Domack, E.W., Kelly, C., 2011. Holocene Southern Ocean surface temperature variability West of the Antarctic Peninsula. Nature 470, 250–254.
- Smellie, J.L., Johnson, J.S., McIntosh, W.C., Esser, R., Gudmundsson, M.G., Hambrey, M.J., van Wyk De Bries, B., 2008. Six million years of glacial history recorded in

- the James Ross Island volcanic group, Antarctic Peninsula. Palaeogeogr. Palaeoclimatol. Palaeoecol. 260, 122–148.
- Stone, J.O., 2000. Air pressure and cosmogenic isotope production. J. Geophys. Res. 105, 23753–23759.
- Strelin, J.A., Malagnino, E.C., 1992. Geomorfología de la isla James Ross. In: Rinaldi, C.A. (Ed.), Geología de la Isla James, Antártida. Instituto Antártico Argentino, Buenos Aires, pp. 7–36.
- Strelin, J., Sone, T., 1998. Rock glaciers on James Ross Island, Antarctica. In: Proceedings of the 7th International Permafrost Conference, pp. 1027–1033.
- Strelin, J.A., Sone, T., Mori, J., Torielli, C.A., Nakamura, T., 2006. New data related to Holocene landform development and climatic change in James Ross Island, Antarctic Peninsula. In: Füterer, D.K., Damaske, D., Kleinschmidt, G., Miller, H., Tessensohn, F. (Eds.), Antarctica: Contributions to Global Earth Sciences. Springer-Verlag, Berlin, pp. 453–458.
- Strelin, J., Kaplan, M., Vandergoes, M., Denton, G., Schaefer, J., 2014. Holocene glacier chronology of the Lago Argentino basin, Southern Patagonian Icefield. Quat. Sci. Rev. 101, 124–145.
- Toggweiler, J.R., Russell, J.L., 2008. Ocean circulation in a warming climate. Nature 451, 286–288.
- Yuan, X., Kaplan, M., Cane, M., 2018. The interconnected global climate system a review of tropical-polar teleconnection. J. Climate 31, 5765–5792.
- Zale, R., Karlen, W., 1989. Lake sediment cores from the Antarctic Peninsula and surrounding islands. Geogr. Ann. 71 (A), 211–220.

1	Supplementary Tables and Analyses
2	
3	
4	Holocene glacier behavior around the northern Antarctic Peninsula
5	and possible causes
6	
7	Kaplan, M.R. <sup>1</sup> , Strelin, J.A. <sup>2,3</sup> , Schaefer, J.M. <sup>1,4</sup> ; Peltier, C. <sup>1,4</sup> , Martini, M.A. <sup>3,5,6</sup> , Flores, E <sup>3</sup> , Winckler,
8	G. <sup>1,4</sup> , Schwartz, R. <sup>1</sup> ,
9	Geochemistry, Lamont-Doherty Earth Observatory, Palisades, NY 10964, USA
10	<sup>2</sup> Instituto Antártico Argentino, <sup>3</sup> Centro de Investigaciones en Ciencias de la Tierra (CICTERRA, CONICET-
11 12	Facultad de Ciencias Exactas, Físicas y Naturales, UNC), Córdoba, Argentina <sup>4</sup> Department of Earth and Environmental Sciences, Columbia University, New York, NY 10027, USA
13	<sup>5</sup> Núcleo Milenio Paleoclima, Universidad de Chile, Santiago, Chile
$\frac{14}{5}$	<sup>6</sup> Instituto de Geografía, Pontificia Universidad Católica de Chile, Santiago, Chile
16	*Corresponding author: Kaplan, mkaplan@ldeo.columbia.edu
17	Keywords: Antarctic Peninsula; cosmogenic dating; deglaciation; Holocene; Antarctica; paleoclimate
18	

Table S1. Surface-exposure sample details and <sup>10</sup>Be data from James Ross and Long Islands

Sample ID	Latitude	Longitude	Elev.	Sample	Shielding	Quartz	<sup>9</sup> Be	$^{10}$ Be/ $^{9}$ Be $\pm 1_{\circ}$	$[^{10}\text{Be}] \pm 1_{\text{G}}$	Age	Context
	(DD)	(DD)	(m asl)	Thickness		mass	added		(atoms g <sup>-1</sup> )	$\pm 1_{\sigma}$	
				(cm)		(g)	(mg)				
LI-13-01	-63.7609	-58.1781	91	2.89	1	10.0915	0.1887	$30.8917 \pm 1.0743$	$38194 \pm 1328$	$7410 \pm 260$	Erratic (retreat)
LI-13-02	-63.7608	-58.1785	91	2.70	1	10.0466	0.1894	$30.5403 \pm 0.9816$	$38071 \pm 1224$	$7370 \pm 240$	Erratic (retreat)
LI-13-03	-63.7610	-58.1792	94	3.02	1	10.0303	0.1892	$43.5831 \pm 2.5205$	54538 ± 3154	$10600 \pm 610$	Erratic (retreat)
LI-13-04	-63.7611	-58.1792	94	2.81	1	10.0270	0.1883	34.0994 ± 1.0808	$42381 \pm 1343$	$8190 \pm 260$	Erratic (retreat)
LI-13-05	-63.7615	-58.1782	95	2.98	1	10.0364	0.1890	$42.7172 \pm 1.1705$	$53355 \pm 1462$	$10300 \pm 280$	Erratic (retreat)
LI-13-06	-63.7615	-58.1783	93	2.23	1	10.2555	0.1894	$33.8098 \pm 1.0260$	$41332 \pm 1254$	$7960 \pm 240$	Erratic (retreat)
BLK1-2014Jul							0.1899	$0.3340 \pm 0.2041$			
SEY-13-01	-64.2437	-56.6561	208	2.17	1	10.2657	0.1901	$18.5529 \pm 0.9426$	22547 ± 1146	$3860 \pm 200$	Erratic (retreat)
SEY-13-02	-64.2467	-56.6527	206	0.82	1	8.8428	0.1911	$22.0009 \pm 0.8137$	$31301 \pm 1158$	$5310 \pm 200$	Erratic (retreat)
SEY-13-04	-64.2580	-56.6522	202	0.89	1	10.3701		44.9864 ± 1.2019	54733 ± 1462	9340 ± 250	Erratic (retreat)
IRQ-13-08	-63.9163	-58.3013	44	0.91	0.9998		0.1894	$32.2033 \pm 0.9788$	$41194 \pm 1252$	$8280 \pm 250$	Erratic (retreat)
JRQ-13-09	-63.9202	-58.3033	38	1.14	0.9997	9.6979	0.1896	29.0290 ± 1.3436	$37657 \pm 1743$	$7630 \pm 350$	Erratic (retreat)
JRQ-13-10	-63.9172	-58.3056	39	1.13	0.9998	20.0370	0.1893	59.7007 ± 1.6442	$37568 \pm 1035$	$7600 \pm 210$	Erratic (retreat)
JRQ-13-24	-63.9237	-58.3012	56	1.52	0.9995	20.0247	0.1901	76.4059 ± 2.0632	48333 ± 1305	9640 ± 260	Erratic (retreat)
JRQ-13-27	-63.9197	-58.3074	31	0.88	0.9998	13.9425	0.1896	46.4459 ± 1.1825	$42028 \pm 1070$	$8560 \pm 220$	Erratic (retreat)
BLK1-2014No							0.1896	$0.3520 \pm 0.1123$			
JRQ-13-25	-63.9193	-58.2972	54	1.99	0.9995	4.0844		18.1462 ± 0.8350	$46314 \pm 2131$	$9290 \pm 430$	Erratic (retreat)
BLK2-2014No	v03						0.1596	$0.1228 \pm 0.4848$			
IRI-14-34	-63.9383	-57.8157	32	3.31	0.9989	20.0267	0.1903	43.8512 ± 0.9529	27714 ± 602.3	5740 ± 130	moraine (expanded)
IRI-14-35	-63.9379	-57.8169	32	2.02	0.9989	12.0831	0.1910	35.4754 ± 0.9966	37261 ± 1047	$7650 \pm 220$	moraine (expanded)
JRI-14-35 JRI-14-36	-63.9379	-57.8142	26	2.02	0.9989	18.1548	0.1916	46.7258 ± 2.2936	$3/201 \pm 104/$ $32818 \pm 1611$	$6790 \pm 330$	moraine (expanded)
JRI-14-30 JRI-14-44	-63.9957	-57.8142	12	1.01	0.9975	12.3542		32.3395 ± 1.5833	33258 ± 1628	$6940 \pm 340$	moraine (expanded)
JRI-14-45	-63.9961	-57.8139	15.4	3.84	0.9979	20.0300		46.2877 ± 1.1648	29417 ± 740.2	$6260 \pm 160$	moraine (expanded)
BLK1-2015Dec		57.0157	13.1	5.51	0.2217	20.0300	0.1917	$0.2078 \pm 0.1057$	27117 11012	0200 100	(e.panded)
JRI-14-01	-64.1091	-58.4023	68	3.85	0.9951	12.9372	0.1917	19.0936 ± 0.7019	18506 ± 680.3	3720 ± 140	moraine (expanded)
JRI-14-01 JRI-14-02	-64.1083	-58.4009	74	3.37	0.9931	20.0757	0.1917	11.7500 ± 0.5648	7231 ± 347.6	$1440 \pm 70$	moraine (expanded)
JRI-14-08	-64.0928	-58.4117	71	2.39	0.9974	20.0206		25.5859 ± 0.8429	16122 ± 531.1	$3190 \pm 110$	Erratic (retreat)
BLK1-2016Jan		50.4117	,,	2.37	0.5574	20.0200	0.1919	$0.4061 \pm 0.1320$	10122 331.1	3130 110	Litato (tetreat)
IRSM-13-43	-63.9385	-57.8191	30	2.09	0.9998	10.5224	0.1909	15.9173 ± 0.9458	19105 ± 1135	3930 ± 230	moraine (expanded)
JRSM-13-38	-63.9540	-57.8424	55	1.86	0.9990	7.6260	0.1914	24.7446 ± 0.8469	41225 ± 1411	$8250 \pm 280$	moraine (expanded)
JRI-14-46	-63.9961	-57.8140	15.4	1.86	0.9979	6.7598	0.1909	18.5632 ± 1.0347	34734 ± 1936	7290 ± 410	moraine (expanded)
JRI-14-09	-64.0926	-58.4133	64	1.97	0.9968	7.4047	0.1909	14.9426 ± 0.6983	25468 ± 1190	5060 ± 240	Erratic (retreat)
JRI-14-11	-64.1160	-58.4508	52	1.61	0.9983	15.2186	0.1920	70.2143 ± 1.3991	59070 ± 1177	$11900 \pm 240$	Erratic (retreat)
JRI-14-13	-64.1161	-58.4497	58	2.62	0.9983	17.0032	0.1918	54.3036 ± 1.4059	40816 ± 1057	8200 ± 210	Erratic (retreat)
BLK-2016May		5011157	20	2.02	0.5505	0.0000		$0.1662 \pm 0.0750$	10010 1007	0200 210	Zitutie (tetreut)
JRI-14-10	-64.0928	-58.4137	57	4.72	0.9968	25.0586	0.1925	29.5066 ± 0.9963	15068 ± 508.8	$3080 \pm 100$	Erratic (retreat)
JRI-14-14	-64.1150	-58.4457	49	3.13	0.9968	22.8175	0.1920	39.0390 ± 1.0097	21864 ± 565.5	4450 ± 120	moraine (expanded)
JRI-14-33	-63.9372	-57.8143	28	4.13	0.9990	25.0160		40.1442 ± 1.0154	20453 ± 517.3	4280 ± 110	moraine (expanded)
											(
JRSM-13-39	-63.9541	-57.8425	52	1.97	0.9989	12.8944	0.1875	$11.7865 \pm 0.5995$	$10395 \pm 528.7$	$2090 \pm 110$	moraine (expanded)
JRSM-13-42	-63.9380	-57.8231	38	0.82	0.9998	5.3437	0.1881	$4.6313 \pm 0.3959$	8338 ± 712.7	$1680 \pm 140$	moraine (expanded)
JRI-14-07	-64.0929	-58.4110	70	1.42	0.9974	11.4510	0.1879	24.9646 ± 0.9194	26188 ± 964.5	$5150 \pm 190$	Erratic (retreat)
JRI-14-17	-64.0926	-58.4133	62	4.80	0.9968	13.5704	0.1878	19.6163 ± 0.9528	$17138 \pm 832.4$	$3480 \pm 170$	Erratic (retreat)
JRI-14-18	-64.0868	-58.4018	142	4.80	0.9785	20.1894	0.1873	40.5527 ± 1.4495	24468 ± 874.5	4660 ± 170	moraine (expanded)
JRI-14-21	-64.0868	-58.4018	143	5.74	0.9785	20.1086	0.1880	36.3546 ± 1.0730	22040 ± 650.5	4220 ± 130	moraine (expanded)
JRI-14-22	-64.1083	-58.4010	72	2.90	0.9941	21.3723	0.1876	16.1193 ± 1.1723	8817 ± 641.3	1750 ± 130	moraine (expanded)
JRI-14-23	-64.1084	-58.3996	74	2.31	0.9941	20.0064		30.1681 ± 0.9077	18266 ± 549.6	3610 ± 110	moraine (expanded)
JRI-14-24	-64.1113	-58.4052	101	1.69	0.9953	20.0206		41.1121 ± 1.4266	25024 ± 868.3		moraine (expanded)
JRI-14-32	-63.9540	-57.8423	54	3.15	0.9994	15.3294		18.0627 ± 0.8677	13915 ± 668.5		moraine (expanded)
BLK1-2016Jun				-			0.1883	1.0864 ± 0.1984			/
IRI-14-15	-64.1151	-58.4468	54	5.43	0.9968	28.3986	0.1885	43.1234 ± 1.6382	18815 ± 714.7	3870 ± 150	moraine (expanded)
JRI-14-19	-64.0868	-58.4018	148	3.72	0.9785	30.1692	0.1884	60.5018 ± 2.2579	24954 ± 931.3	4680 ± 180	moraine (expanded)
JRI-14-25	-64.1112	-58.4057	101	3.60	0.9940	25.0785	0.1889	47.1809 ± 1.3786	$23396 \pm 683.6$	4540 ± 130	moraine (expanded)
JRI-14-26	-64.1113	-58.4057	93	3.71	0.9940	26.1183	0.1887	37.7443 ± 1.2207	17883 ± 578.3	3500 ± 110	moraine (expanded)
JRI-14-47	-63.9961	-57.8140	15.4	3.31	0.9979	14.3477		28.2201 ± 0.9645	24140 ± 825.1	5100 ± 170	moraine (expanded)
BLK1-2016Au		27.0170	15.7	5.51	5.7717	21.37//	0.1885	$0.7119 \pm 0.4409$	2.1.10 023.1	5100 170	(expanded)
JRI-14-27	-64.0999	-58.4200	53	4.11	0.9991	69.9398	0.1889	9.1881 ± 0.4755	1512 ± 78.27	310 ± 20	moraine (expanded)
IRI-14-28	-64.0999	-58.4191	56	3.66	0.9989	70.2921	0.1890	$7.1068 \pm 0.4480$	$1132 \pm 71.33$	$230 \pm 10$	moraine (expanded)
JRI-14-29	-64.1016	-58.4103	47	3.88	0.9985	70.2478	0.1887	$3.9966 \pm 0.3383$	$571.8 \pm 48.40$	$120\pm10$	supraglacial debris/thrust rid
JRI-14-30	-64.1002	-58.4157	42	4.36	0.9980	63.3855	0.1884	$3.3120 \pm 0.3992$	$496.4 \pm 59.84$	$100 \pm 10$	ice edge/pond coverage?
BLK2-2016Au							0.1886	$0.8120 \pm 0.1796$			<b>-</b>
	pt05						0.187527	0.6090 ± 0.1305			
BLK1-2017-Se	-63.95219	-57.86201	90	5.45	0.9983	70.1901	0.188249	12.7349 ± 0.6253	$2138 \pm 105.0$	$420 \pm 20$	end of left lateral/ice edge
JRI-14-41		-57 86125	5 93	3.13	0.9970	70 1065	0.18/115	0.0952 ± 0.6095	944.1 ± 94 /1	180 ± 70	supraglacial debris/thriist rid
BLK1-2017-Se JRI-14-41 JRI-14-42 IRI-14-43	-63.95265	-57.86125		3.13 4.37	0.9970		0.187115	$6.0952 \pm 0.6095$ $3.6400 \pm 0.4298$	942.1 ± 94.21 499.3 ± 58.95	180 ± 20 100 ± 10	
JRI-14-41		-57.86125 -57.85955 -57.85667	5 93 66 77	3.13 4.37 4.55	0.9970 0.9970 0.9997	70.8324	0.187115 0.187218 0.187321	3.6400 ± 0.4298 5.4783 ± 0.4823	499.3 ± 58.95 1099 ± 96.78	$180 \pm 20$ $100 \pm 10$ $220 \pm 20$	supraglacial debris/thrust rid moraine (expanded) moraine (expanded)

Notes for Table S1: We processed procedural blanks identically to the samples, with one or two blanks accompanying each sample batch, respectively, as indicated in table. AMS standard used for normalization is 2.85x 10<sup>-12</sup> = 07KNSTD3110. Shown are 1σ analytical AMS uncertainties. Column of <sup>9</sup>Be added is adjusted for carrier (Be) concentration. Elevations are measured with a hand held Garmin. In addition, for all samples at Dreadnought (JRI-14-44 to -47) we used a hand level to measure elevation above mean high tide. The context column matches that (red and blue for retreat and expanded, respectively) on Figures 2 to 6. As explained in the text, we used version 2.2 with version 2.2.1 of the constants file (Balco et al., 2008) with a high-resolution version of the geomagnetic framework (Lifton et al., 2008), and we show ages with Lm scaling. Choice of scaling model and the version of the online calculator do not affect our inferences and conclusions (see text).

Table also provided as Supplementary spreadsheet Table S1.

Table S2. <sup>10</sup>Be ages by location

14010 521	De ages 2, 10		Maximum haiah
Long Island			Maximum height (cm)
LI-13-01	$7410 \pm 260$	Erratic (retreat)	cobble
LI-13-01 LI-13-02	$7370 \pm 240$	Erratic (retreat)	cobble
LI-13-03	$10600 \pm 610$	Erratic (retreat)	cobble
LI-13-04	$8190 \pm 260$	Erratic (retreat)	cobble
LI-13-05	$10300 \pm 280$	Erratic (retreat)	cobble
LI-13-05 LI-13-06	$7960 \pm 240$	Erratic (retreat)	cobble
LI-13-00	7900 ± 240	Estatic (tetteat)	CODDIC
Seymour Isla	nd (also see Johnso	on et al, 2011)	
SEY-13-01	$3860 \pm 200$	Erratic (retreat)	90
SEY-13-02	$5310 \pm 200$	Erratic (retreat)	50
SEY-13-04	$9340\pm250$	Erratic (retreat)	80-90
La amalina Dam	in on lo		
Lagrelius Pen	8280 ± 250	Francis (notice 4)	120
JRQ-13-08		Erratic (retreat)	120
JRQ-13-09	$7630 \pm 350$	Erratic (retreat)	80 70
JRQ-13-10	$7600 \pm 210$	Erratic (retreat)	
JRQ-13-24	$9640 \pm 260$ $8560 \pm 220$	Erratic (retreat) Erratic (retreat)	50 30
JRQ-13-27		, ,	36
JRQ-13-25	$9290 \pm 430$	Erratic (retreat)	30
Santa Martha	area		
JRI-14-33	4280 ± 110	moraine (expanded)	cobble
JRI-14-34	$5740 \pm 130$	moraine (expanded)	cobble
JRI-14-35	$7650 \pm 220$	moraine (expanded)	10
JRI-14-36	$6790 \pm 330$	moraine (expanded)	7
JRSM-13-43	$3930 \pm 230$	moraine (expanded)	33
JRSM-13-42	$1680\ \pm 140$	moraine (expanded)	5-10
411 GL:			
Alpha Glacier	=		
JRSM-13-38	$8250 \pm 280$	moraine (expanded)	cobble
JRSM-13-39	2090 110	moraine (expanded)	cobble
JRI-14-32	$2810 \pm 140$	moraine (expanded)	cobble
JRI-14-41	$420 \pm 20$	end of left lateral/ice edge	cobble
JRI-14-42	$180 \pm 20$ $100 \pm 10$	supraglacial debris/thrust ridge	cobble
JRI-14-43 JRI-14-50	$100 \pm 10$ $220 \pm 20$	moraine (expanded)	cobble cobble
JKI-14-30	220 ± 20	moraine (expanded)	cobble
Dreadnought	<u> </u>		
JRI-14-44	$6940 \pm 340$	moraine (expanded)	57
JRI-14-45	$6260 \pm 160$	moraine (expanded)	cobble
JRI-14-46	$7290 \pm 410$	moraine (expanded)	cobble
JRI-14-47	$5100\ \pm 170$	moraine (expanded)	cobble
Rhum Glacier JRI-14-01	3720 ± 140	moraine (expanded)	cobble
JRI-14-01 JRI-14-02	$1440 \pm 70$	moraine (expanded)	cobble
JRI-14-02 JRI-14-07	$5150 \pm 190$	Erratic (retreat)	20
JRI-14-08	$3190 \pm 110$	Erratic (retreat)	10
JRI-14-09	$5060 \pm 240$	Erratic (retreat)	50
JRI-14-10	$3080 \pm 100$	Erratic (retreat)	cobble
JRI-14-11	$11900 \pm 240$	Erratic (retreat)	10
JRI-14-13	$8200 \pm 210$	Erratic (retreat)	cobble
JRI-14-14	$4450 \pm 120$	moraine (expanded)	cobble
JRI-14-15	$3870 \pm 150$	moraine (expanded)	cobble
JRI-14-17	$3480 \pm 170$	Erratic (retreat)	cobble
JRI-14-18	$4660 \pm 170$	moraine (expanded)	cobble
JRI-14-19	$4680 \pm 180$	moraine (expanded)	cobble
JRI-14-21	$4220 \pm 130$	moraine (expanded)	cobble
JRI-14-22	$1750 \pm 130$	moraine (expanded)	cobble
JRI-14-23	$3610 \pm 110$	moraine (expanded)	cobble
JRI-14-24	$4780 \pm 170$	moraine (expanded)	cobble
JRI-14-25	$4540 \pm 130$	moraine (expanded)	cobble
JRI-14-26	$3500 \pm 110$	moraine (expanded)	cobble
JRI-14-27	$310 \pm 20$	moraine (expanded)	cobble
JRI-14-28	$230 \pm 10$	moraine (expanded)	cobble
JRI-14-29	$120 \pm 10$	supraglacial debris/thrust ridge	cobble
JRI-14-30	$100 \pm 10$	ice edge/pond coverage?	cobble
		<i>5</i> 1 <i>6</i>	

Notes: Cobbles are typically less than 5 cm high; see thickness in Table S1. Four samples in italics are on sandstone concretions; these are notably younger than the rest of the samples from the same landform in each respective area, and we assume they are outliers in the probability distributions (Figures 4-6, and S1).

## Table also provided as Supplementary spreadsheet Table S2.

Table S3. 10 Be	from prior studies o	on James Ross Island (Lm scaling)
LAC-02	$9600 \pm 390$	Johnson et al. (2011)
LAC-03	$9800~\pm~390$	Johnson et al. (2011)
LAC-04	$12900~\pm~520$	Johnson et al. (2011)
LAC-05	$10000~\pm~530$	Johnson et al. (2011)
SEY-01	$9000~\pm~410$	Johnson et al. (2011)
SEY-02	$9900~\pm~390$	Johnson et al. (2011)
SEY-03	$14300~\pm~550$	Johnson et al. (2011)
SEY-04	$29700  \pm  1090$	Johnson et al. (2011)
JOH-01	$37500~\pm~1340$	Johnson et al. (2011)
JOH-02	$9700~\pm~380$	Johnson et al. (2011)
JOH-04	$8000~\pm~370$	Johnson et al. (2011)
JOH-05	$30400~\pm~950$	Johnson et al. (2011)
TER-04	$8100 \pm 340$	Johnson et al. (2011)
TER-05	$10900~\pm~490$	Johnson et al. (2011)
TER-07	$9100~\pm~440$	Johnson et al. (2011)
TER-08	$10300~\pm~440$	Johnson et al. (2011)
JRI03	$12700~\pm~530$	Glasser et al. (2014)
JR01	$14600~\pm~520$	Glasser et al. (2014)
JRI09	$10500~\pm~380$	Glasser et al. (2014)
JRI26	$7600~\pm~410$	Glasser et al. (2014)
JRI29	$7400~\pm~440$	Glasser et al. (2014)
JRI35	$7300~\pm~300$	Glasser et al. (2014)
JRI49	$21700~\pm~1060$	Glasser et al. (2014)
JRI50	$16900~\pm~750$	Glasser et al. (2014)
JRI62	$8700 \pm 350$	Glasser et al. (2014)
DN05-001	$13000~\pm~2550$	Nývlt et al. (2014)
DN07-005	$19200~\pm~1090$	Nývlt et al. (2014)
DN07-077	$15100~\pm~900$	Nývlt et al. (2014)
DN07-078	$16000~\pm~860$	Nývlt et al. (2014)
DN07-079	$15300~\pm~780$	Nývlt et al. (2014)
DN07-080	$22500~\pm~1270$	Nývlt et al. (2014)
DN07-081	$15900~\pm~700$	Nývlt et al. (2014)
DN09-111	$26600~\pm~4170$	Nývlt et al. (2014)
DN09-091	$30200 \pm 5230$	Nývlt et al. (2014)

Table also provided as Supplementary spreadsheet Table S3.

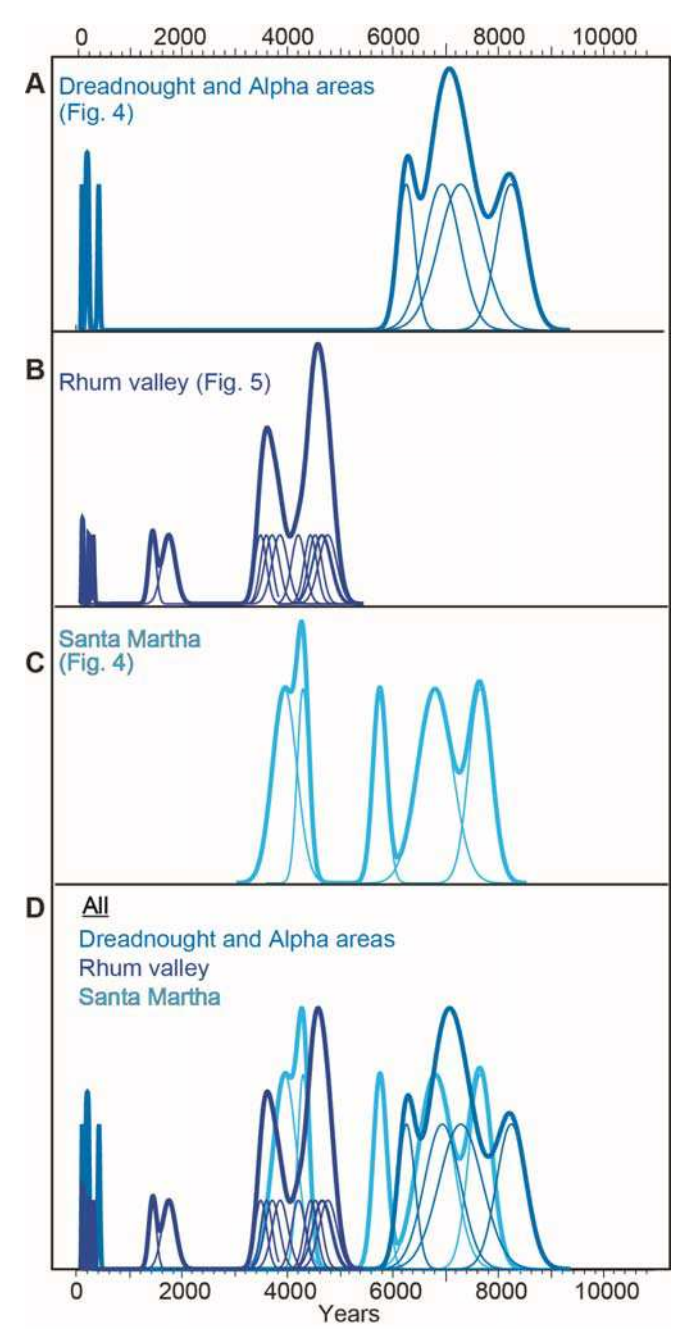


Figure S1. Probability distribution plots of moraine ages for Dreadnought and Alpha area (**A**), Rhum valley (**B**), Santa Martha (**C**), and all sites together (**D**). Individual <sup>10</sup>Be ages are shown by thin curves with 1σ uncertainties. The thick lines represents the probability distribution of the respective age population. Y-axis is relative probability and standardized to 1. Only one moraine crest (i.e., former glacier limit) is at Dreadnought (**A**), which affords three relatively coherent middle Holocene <sup>10</sup>Be ages (~7-6 ka). No glacier has existed at Santa Martha (**C**) since the middle Holocene, and thus younger moraines there did not form. Santa Martha perhaps contains the largest age scatter, given there is only major morainal landform. Perhaps it is a compound feature representing more than one glacier advance, as notably the Santa Martha ages overlap within uncertainties with the moraine ages at the other 3 sites; or some boulders instead represent glacier recession (see text); We do not include outliers, discussed in the text, such as the sandstone erratics.

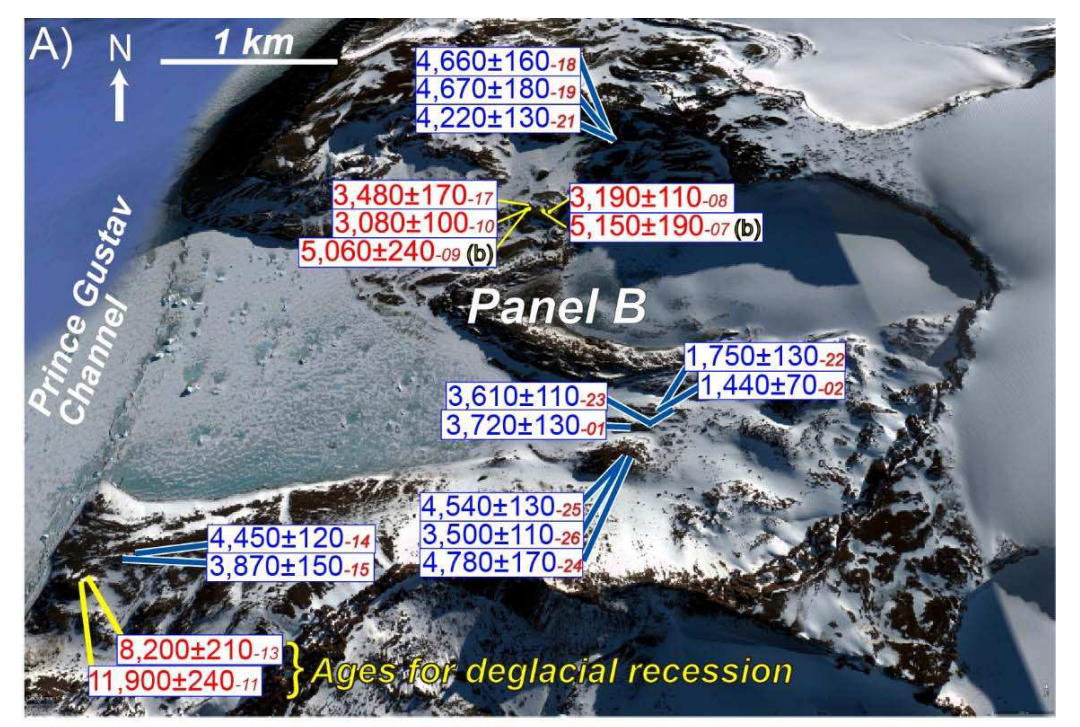




Figure S2. Following Figure 5, a focus on the Rhum area, with bottom panel showing the front of the glacier. Ages overlie a Google Earth image. Red and blue labels, represent erratics left behind and lateral moraine samples, respectively, and follow convention throughout the paper. The last two digits refers to the sample label (Tables S1, S2). The 'b' after -07 and -09 labels represent samples are from a boulder (Table S1). Whereas the ages of  $310\pm20$  and  $230\pm10$  yrs date moraine samples, the two innermost ages (-30 and -29) are associated with debris bands sitting by the glacier front.